Chapter 8
Asymptotic Safety, Fractals, and Cosmology

Martin Reuter and Frank Saueressig

Abstract These lecture notes introduce the basic ideas of the asymptotic safety approach to quantum Einstein gravity (QEG). In particular they provide the background for recent work on the possibly multi-fractal structure of the QEG spacetimes. Implications of asymptotic safety for the cosmology of the early Universe are also discussed.

8.1 Introduction

Finding a consistent and fundamental quantum theory for gravity is still one of the most challenging open problems in theoretical high-energy physics to date. As is well known, the perturbative quantization of the classical description for gravity, general relativity, results in a non-renormalizable quantum theory [1–3]. One possible lesson drawn from this result may assert that gravity constitutes an effective field theory valid at low energies, whose ultraviolet (UV) completion requires the introduction of new degrees of freedom and symmetries. This is the path followed, e.g., by string theory. In a less radical approach, one retains the fields and symmetries known from general relativity and conjectures that gravity constitutes a fundamental theory at the non-perturbative level. One proposal along this line is the asymptotic safety scenario [4–6] initially put forward by Weinberg [7–10]. The key ingredient in this scenario is a non-Gaussian fixed point (NGFP) of the gravitational renormalization group (RG) flow, which controls the behavior of the theory at high energies and renders physical quantities safe from unphysical divergences. Given that the NGFP comes with a finite number of unstable (or relevant) directions, this construction is as predictive as a 'standard' perturbatively renormalizable quantum field theory.

M. Reuter (✉) · F. Saueressig
Institute of Physics, University of Mainz, Staudingerweg 7, 55099 Mainz, Germany
e-mail: reuter@thep.physik.uni-mainz.de

F. Saueressig
e-mail: saueressig@thep.physik.uni-mainz.de

G. Calcagni et al. (eds.), *Quantum Gravity and Quantum Cosmology*,
Lecture Notes in Physics 863, DOI 10.1007/978-3-642-33036-0_8,

(1) The primary tool for investigating this scenario is the functional renormalization group equation (FRGE) for gravity [11], which constitutes the spring-board for the detailed investigations of the non-perturbative renormalization group behavior of quantum Einstein gravity [11–60]. The FRGE defines a Wilsonian RG flow on a theory space which consists of all diffeomorphism-invariant functionals of the metric $g_{\mu\nu}$, and turned out to be ideal for investigating the asymptotic safety conjecture [4–8]. In fact, it yielded substantial evidence for the non-perturbative renormalizability of quantum Einstein gravity. The theory emerging from this construction (henceforth denoted 'QEG') is not a quantization of classical general relativity. Instead, its bare action corresponds to a non-trivial fixed point of the RG flow and is a prediction therefore.

The approach of [11] employs the effective average action Γ_k [61–72] which has crucial advantages as compared to other continuum implementations of the Wilsonian RG flow [73–76]. The scale dependence of Γ_k is governed by the FRGE [61]

$$k\partial_k\Gamma_k[\Phi,\bar{\Phi}] = \frac{1}{2}\mathrm{STr}\left[\left(\frac{\delta^2\Gamma_k}{\delta\Phi^A\delta\Phi^B}+\mathscr{R}_k\right)^{-1}k\partial_k\mathscr{R}_k\right]. \tag{8.1}$$

Here Φ^A is the collection of all dynamical fields considered, $\bar{\Phi}^A$ denotes their background counterparts and STr denotes a generalized functional trace carrying a minus sign for fermionic fields and a factor 2 for complex fields. Moreover $\mathscr{R}_k$ is a matrix-valued infrared cutoff, which provides a k-dependent mass-term for fluctuations with momenta $p^2 \ll k^2$, while vanishing for $p^2 \gg k^2$. Solutions of the flow equation give rise to families of effective field theories $\{\Gamma_k[g_{\mu\nu}], 0 \leq k < \infty\}$ labeled by the coarse-graining scale k. The latter property opens the door to a rather direct extraction of physical information from the RG flow, at least in single-scale cases: If the physical process under consideration involves a single typical momentum scale p_0 only, it can be described by a tree-level evaluation of $\Gamma_k[g_{\mu\nu}]$, with $k = p_0$.

(2) Already soon after the asymptotic safety program had taken its modern form, various indications pointed in the direction that in QEG space-time should have certain features in common with a fractal. In ref. [13] the four-dimensional graviton propagator has been studied in the regime of asymptotically large momenta and it has been found that near the Planck scale a kind of dynamical dimensional reduction occurs. As a consequence of the NGFP controlling the UV behavior of the theory, the four-dimensional graviton propagator essentially behaves as two-dimensional on microscopic scales.

Subsequently, the "finger prints" of the NGFP on the fabric of the effective QEG space-times have been discussed in [15], where it was shown that asymptotic safety induces a characteristic self-similarity of space-time on length scales below the Planck length ℓ_{Pl}. The graviton propagator becomes scale-invariant in this regime [13]. Based on this observation it was argued that, in a cosmological context, the geometry fluctuations it describes can give rise to a scale-free spectrum of primordial density perturbations responsible for structure formation [77–81]. Thus the overall picture of the space-time structure in asymptotically safe gravity as it emerged about

ten years ago comprises a smooth classical manifold on large distance scales, while on small scales one encounters a low-dimensional effective fractal [13, 15].

The characteristic feature at the heart of these results is that the effective field equations derived from the gravitational average action equip every given smooth space-time manifold with, in principle, infinitely many different (pseudo-) Riemannian structures, one for each coarse-graining scale [82, 83]. Thus, very much like in the famous example of the coast line of England [84], the proper length on a QEG space-time depends on the 'length of the yardstick' used to measure it. Earlier on similar fractal properties had already been found in other quantum gravity theories, in particular near dimension 2 [85], in a non-asymptotically safe model [86] and by analyzing the conformal anomaly [87].

Along a different line of investigations, the causal dynamical triangulation (CDT) approach has been developed and first Monte-Carlo simulations were performed [88–95]; see [96] for a recent review. In this framework one attempts to compute quantum gravity partition functions by numerically constructing the continuum limit of an appropriate statistical mechanics system. This limit amounts to a second-order phase transition. If CDT and its counterpart QEG, formulated in the continuum by means of the average action, belong to the same universality class, one may expect that the phase transition of the former is described by the non-trivial fixed point underlying the asymptotic safety of the latter.

Remarkably, ref. [90–92] reported results which indicated that the four-dimensional CDT space-times, too, undergo a dimensional reduction from four to two dimensions as one 'zooms' in on short distances. In particular, it had been demonstrated that the spectral dimension d_s measured in the CDT simulations has the very same limiting behaviors, $4 \to 2$, as in QEG [97]. Therefore it was plausible to assume that both approaches indeed 'see' the same continuum physics.

This interpretation became problematic when ref. [94] carried out CDT simulations for $d = 3$ macroscopic dimensions, which favor a value near $d_s = 2$ on the shortest length-scale probed since, in this case, the QEG prediction for the fixed point region is the value $d_s = 3/2$ [97]. Furthermore, the authors of ref. [98] reported simulations within the *Euclidean* dynamical triangulation (EDT) approach in $d = 4$, which favor a drop of the spectral dimension from 4 to about 1.5; this is again in conflict with the QEG expectations if one interprets the latter dimension as the value in the continuum limit.

Later on we will present several types of scale-dependent effective dimensions, specifically the spectral dimension d_s and the walk dimension d_w for the effective QEG space-times. We shall see that on length scales slightly *larger* than $\ell_{\rm Pl}$ there exists a further regime which exhibits the phenomenon of dynamical dimensional reduction. There the spectral dimension is even smaller than near the fixed point, namely $d_s = 4/3$ in the case of 4 dimensions classically. Moreover, we shall argue that the (3-dimensional) results reported in [94] are in perfect accord with QEG, but that the shortest possible length scale achieved in the simulations is not yet close to the Planck length. Rather, the Monte Carlo data probe the transition between the classical and the newly discovered 'semi-classical' regime [99].

For similar work on fractal features in different approaches we must refer to the literature [100–122].

(3) As for possible physics implications of the RG flow predicted by QEG, ideas from particle physics, in particular the 'RG improvement', have been employed in order to study the leading quantum gravity effects in black holes [123–126], cosmological space-times [77–81, 127–136] or possible observable signatures from asymptotic safety at the LHC [137–140]. Among other results, it was found [123–125] that the quantum effects tend to decrease the Hawking temperature of black holes, and that their evaporation process presumably stops completely once the black holes mass is of the order of the Planck mass. In cosmology it turned out that inflation can occur without the need of an inflaton, and that the running of the cosmological constant might be responsible for the observed entropy of the present Universe [79–81].

These lectures are intended to provide the necessary background for these developments. They consist of three main parts, dealing with the basic ideas of asymptotic safety, the fractal QEG space-times, and possible implications of asymptotic safety for cosmology, respectively.

8.2 Theory Space and Its Truncation

We start by reviewing the basic ideas underlying asymptotic safety, referring to [4–6] for a more detailed discussion. The arena in which the Wilsonian RG dynamics takes place is 'theory space'. Albeit a somewhat formal notion, it helps in visualizing various concepts related to functional renormalization group equations; see Fig. 8.1. To describe it, we shall consider an arbitrary set of fields $\Phi(x)$. Then the corresponding theory space consists of all (action) functionals $A : \Phi \mapsto A[\Phi]$ depending on this set, possibly subject to certain symmetry requirements (a $\mathbb{Z}_2$-symmetry for a single scalar, or diffeomorphism invariance if Φ denotes the space-time metric, for instance). So the theory space $\{A[\cdot]\}$ is completely determined once the field content and the symmetries are fixed. Let us assume we can find a set of 'basis functionals' $\{P_\alpha[\cdot]\}$ so that every point of theory space has an expansion of the form

$$A[\Phi, \bar{\Phi}] = \sum_{\alpha=1}^{\infty} \bar{u}_\alpha P_\alpha[\Phi, \bar{\Phi}]. \tag{8.2}$$

The basis $\{P_\alpha[\cdot]\}$ will include both local field monomials and non-local invariants and we may use the 'generalized couplings' $\{\bar{u}_\alpha, \alpha = 1, 2, \ldots\}$ as local coordinates. More precisely, the theory space is coordinatized by the subset of 'essential couplings', i.e., those coordinates which cannot be absorbed by a field reparameterization.

Geometrically speaking the FRGE for the effective average action, Eq. (8.1), defines a vector field β on theory space. The integral curves along this vector field are the 'RG trajectories' $k \mapsto \Gamma_k$ parameterized by the scale k. They start, for $k \to \infty$, at the microscopic action S and terminate at the ordinary effective action at

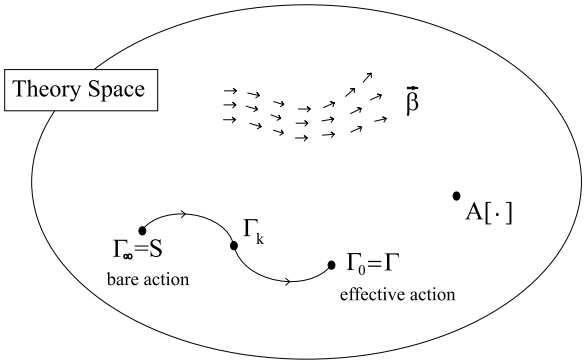

Fig. 8.1 The points of theory space are the action functionals $A[\cdot]$. The RG equation defines a vector field β on this space; its integral curves are the RG trajectories $k \mapsto \Gamma_k$. They emanate from the fixed point action $\Gamma_* \equiv \Gamma_\infty$, which might differ from the bare action by a simple explicitly known functional, and end at the standard effective action Γ

$k = 0$. The natural orientation of the trajectories is from higher to lower scales k, the direction of increasing 'coarse graining'. Expanding Γ_k as in (8.2),

$$\Gamma_k[\Phi, \bar{\Phi}] = \sum_{\alpha=1}^{\infty} \bar{u}_\alpha(k) P_\alpha[\Phi, \bar{\Phi}], \tag{8.3}$$

the trajectory is described by infinitely many 'running couplings' $\bar{u}_\alpha(k)$. Inserting (8.3) into the FRGE we obtain a system of infinitely many coupled differential equations for the $\bar{u}_\alpha$'s:

$$k\partial_k \bar{u}_\alpha(k) = \overline{\beta}_\alpha(\bar{u}_1, \bar{u}_2, \ldots; k), \quad \alpha = 1, 2, \ldots. \tag{8.4}$$

Here the 'beta functions' $\overline{\beta}_\alpha$ arise by expanding the trace on the right-hand side of the FRGE in terms of $\{P_\alpha[\cdot]\}$, i.e., $\frac{1}{2}\mathrm{Tr}[\cdots] = \sum_{\alpha=1}^{\infty} \overline{\beta}_\alpha(\bar{u}_1, \bar{u}_2, \ldots; k) P_\alpha[\Phi, \bar{\Phi}]$. The expansion coefficients $\overline{\beta}_\alpha$ have the interpretation of beta functions similar to those of perturbation theory, but not restricted to relevant couplings. In standard field theory jargon one would refer to $\bar{u}_\alpha(k = \infty)$ as the 'bare' parameters and to $\bar{u}_\alpha(k = 0)$ as the 'renormalized' or 'dressed' parameters.

The notation with the bar on $\bar{u}_\alpha$ and $\overline{\beta}_\alpha$ is to indicate that we are still dealing with dimensionful couplings. Usually the flow equation is reexpressed in terms of the dimensionless couplings

$$u_\alpha \equiv k^{-d_\alpha} \bar{u}_\alpha, \tag{8.5}$$

where d_α is the canonical mass dimension of $\bar{u}_\alpha$. Correspondingly, the essential u_α's are used as coordinates of theory space. The resulting RG equations

$$k\partial_k u_\alpha(k) = \beta_\alpha(u_1, u_2, \ldots) \tag{8.6}$$

are a coupled system of autonomous differential equations. The β_α's have no explicit k-dependence and define a 'time independent' vector field on theory space.

In this language, the basic idea of renormalization can be understood as follows. The boundary of theory space depicted in Fig. 8.1 is meant to separate points with coordinates $\{u_\alpha, \alpha = 1, 2, \ldots\}$ with all the essential couplings u_α well defined, from

points with undefined, divergent couplings. The basic task of renormalization theory consists in constructing an 'infinitely long' RG trajectory which lies entirely within this theory space, i.e., a trajectory which neither leaves theory space (that is, develops divergences) in the UV limit $k \to \infty$ nor in the infrared (IR) limit $k \to 0$. Every such trajectory defines one possible quantum theory.

The consistent UV behavior can be ensured by performing the limit $k \to \infty$ at a fixed point $\{u^*_\alpha, \alpha = 1, 2, \ldots\} \equiv u^*$ of the RG flow. The fixed point is a zero of the vector field $\beta \equiv (\beta_\alpha)$, i.e., $\beta_\alpha(u^*) = 0$ for all $\alpha = 1, 2, \ldots$. The RG trajectories, solutions of $k\partial_k u_\alpha(k) = \beta_\alpha[u(k)]$, have a low 'velocity' near a fixed point because the β_α's are small there and directly at the fixed point the running stops completely. As a result, one can 'use up' an infinite amount of RG time near/at the fixed point if one bases the quantum theory on a trajectory which runs into such a fixed point for $k \to \infty$. This construction ensures that in the UV limit the trajectory ends at an 'inner point' of theory space giving rise to a well-behaved action functional. Thus we can be sure that, for $k \to \infty$, the trajectory does not develop pathological properties such as divergent couplings. The resulting quantum theory is 'safe' from unphysical divergences.

At this stage it is natural to distinguish two classes of fixed points. First, the UV limit may be performed at a Gaussian fixed point (GFP) where $u^*_\alpha = 0$, $\forall \alpha = 1, 2, \ldots$. In this case, the fixed point functional does not contain interactions and the theory becomes asymptotically free in the UV. This is the construction underlying perturbatively renormalizable quantum field theories. More general, one can also use a non-Gaussian fixed point (NGFP) for letting $k \to \infty$, where, by definition, not all of the coordinates u^*_α vanish. In the context of gravity, Weinberg [7, 8] proposed that the UV limit of the theory is provided by such a NGFP.

Note that at the NGFP it is the *dimensionless* essential couplings (8.5) which assume constant values. Therefore, even directly at a NGFP where $u_\alpha(k) \equiv u^*_\alpha$, the dimensionful couplings keep running according to a power law

$$\bar{u}_\alpha(k) = u^*_\alpha k^{d_\alpha}. \tag{8.7}$$

Furthermore, non-essential dimensionless couplings are not required to attain fixed point values.

Given a fixed point, an important concept is its *UV critical hypersurface* $\mathscr{S}_{\rm UV}$, or synonymously, its *unstable manifold*. By definition, it consists of all points of theory space which are pulled into the fixed point by the inverse RG flow, i.e., for *in*creasing k. Its dimensionality $\dim(\mathscr{S}_{\rm UV}) \equiv \Delta_{\rm UV}$ is given by the number of attractive (for *in*creasing cutoff k) directions in the space of couplings.

For the RG equations (8.6), the linearized flow near the fixed point is governed by the Jacobi matrix $\mathbf{B} = (B_{\alpha\gamma})$, $B_{\alpha\gamma} \equiv \partial_\gamma \beta_\alpha(u^*)$:

$$k\partial_k u_\alpha(k) = \sum_\gamma B_{\alpha\gamma}\big(u_\gamma(k) - u^*_\gamma\big). \tag{8.8}$$

The general solution to this equation reads

$$u_\alpha(k) = u^*_\alpha + \sum_I C_I V^I_\alpha \left(\frac{k_0}{k}\right)^{\theta_I}, \tag{8.9}$$

where the V^I's are the right-eigenvectors of $\mathbf{B}$ with eigenvalues $-\theta_I$, i.e., $\sum_\gamma B_{\alpha\gamma} V^I_\gamma = -\theta_I V^I_\alpha$. Since $\mathbf{B}$ is not symmetric in general the θ_I's are not guaranteed to be real. We assume that the eigenvectors form a complete system though. Furthermore, k_0 is a fixed reference scale, and the C_I's are constants of integration. The quantities θ_I are referred to as *critical exponents* since when the renormalization group is applied to critical phenomena (second-order phase transitions) the traditionally defined critical exponents are related to the θ_I's in a simple way [68, 69].

If $u_\alpha(k)$ is to describe a trajectory in $\mathscr{S}_{\rm UV}$, $u_\alpha(k)$ must approach u^*_α in the limit $k \to \infty$ and therefore we must set $C_I = 0$ for all I with $\mathrm{Re}\,\theta_I < 0$. Hence the dimensionality $\Delta_{\rm UV}$ equals the number of $\mathbf{B}$-eigenvalues with a negative real part, i.e., the number of θ_I's with $\mathrm{Re}\,\theta_I > 0$. The corresponding eigenvectors span the tangent space to $\mathscr{S}_{\rm UV}$ at the NGFP. If we *lower* the cutoff for a generic trajectory with all C_I nonzero, only $\Delta_{\rm UV}$ 'relevant' parameters corresponding to the eigendirections tangent to $\mathscr{S}_{\rm UV}$ grow ($\mathrm{Re}\,\theta_I > 0$), while the remaining 'irrelevant' couplings pertaining to the eigendirections normal to $\mathscr{S}_{\rm UV}$ decrease ($\mathrm{Re}\,\theta_I < 0$). Thus near the NGFP a generic trajectory is attracted towards $\mathscr{S}_{\rm UV}$.

Coming back to the asymptotic safety construction, let us now use this fixed point in order to take the limit $k \to \infty$. The trajectories which define an infinite cutoff limit are special in the sense that all irrelevant couplings are set to zero: $C_I = 0$ if $\mathrm{Re}\,\theta_I < 0$. These conditions place the trajectory exactly on $\mathscr{S}_{\rm UV}$. There is a $\Delta_{\rm UV}$-parameter family of such trajectories, and the experiment must decide which one is realized in Nature. Therefore the predictive power of the theory increases with decreasing dimensionality of $\mathscr{S}_{\rm UV}$, i.e., number of UV attractive eigendirections of the NGFP. If $\Delta_{\rm UV} < \infty$, the quantum field theory thus constructed is comparable to and as predictive as a perturbatively renormalizable model with $\Delta_{\rm UV}$ 'renormalizable couplings'. Summarizing, we call a theory *asymptotically safe* if its UV behavior is controlled by a non-Gaussian fixed point with a finite number of relevant directions. The former condition ensures that the theory is safe from unphysical UV divergences while the latter requirement guarantees the predictivity of the construction.

Up to this point our discussion did not involve any approximation. A method which gives rise to non-perturbative approximate solutions is to truncate the theory space $\{A[\cdot]\}$. The basic idea is to project the RG flow onto a finite-dimensional subspace of theory space. The subspace should be chosen in such a way that the projected flow encapsulates the essential physical features of the exact flow on the full space.

Concretely, the projection onto a truncation subspace is performed as follows. One makes an ansatz of the form $\Gamma_k[\Phi, \bar{\Phi}] = \sum_{i=1}^N \bar{u}_i(k) P_i[\Phi, \bar{\Phi}]$, where

the k-independent functionals $\{P_i[\cdot], i = 1, \ldots, N\}$ form a 'basis' on the subspace selected. For a scalar field ϕ, say, examples include pure potential terms $\int d^dx\phi^m(x)$, $\int d^dx\phi^n(x)\ln\phi^2(x), \ldots$, a standard kinetic term $\int d^dx(\partial\phi)^2$, higher order derivative terms $\int d^dx\,\phi(\partial^2)^n\phi$, $\int d^dx\, f(\phi)(\partial^2)^n\phi(\partial^2)^m\phi, \ldots$, and non-local terms like $\int d^dx\,\phi\ln(-\partial^2)\phi, \ldots$. Even if Γ_∞ is simple, a standard ϕ^4 action, say, the evolution from $k = \infty$ downwards will generate such terms.

The projected RG flow is described by a set of ordinary (if $N < \infty$) differential equations for the couplings $\bar{u}_i(k)$. They arise as follows. Let us assume we expand the Φ-dependence of $\frac{1}{2}\mathrm{Tr}[\cdots]$ (with the ansatz for $\Gamma_k[\Phi, \bar{\Phi}]$ inserted) in a basis $\{P_\alpha[\cdot]\}$ of the *full* theory space which contains the P_i's spanning the truncated space as a subset:

$$\begin{aligned}\frac{1}{2}\mathrm{Tr}[\cdots] &= \sum_{\alpha=1}^{\infty}\overline{\beta}_\alpha(\bar{u}_1, \ldots, \bar{u}_N; k)P_\alpha[\Phi, \bar{\Phi}] \\ &= \sum_{i=1}^{N}\overline{\beta}_i(\bar{u}_1, \ldots, \bar{u}_N; k)P_i[\Phi, \bar{\Phi}] + \text{rest}. \end{aligned} \tag{8.10}$$

Here the 'rest' contains all terms outside the truncated theory space; the approximation consists in neglecting precisely those terms. Thus, equating (8.10) to the LHS of the flow equation, $\partial_t\Gamma_k = \sum_{i=1}^{N}\partial_t\bar{u}_i(k)P_i$, the linear independence of the P_i's implies the coupled system of ordinary differential equations

$$\partial_t\bar{u}_i(k) = \overline{\beta}_i(\bar{u}_1, \ldots, \bar{u}_N; k), \quad i = 1, \ldots, N. \tag{8.11}$$

Solving (8.11) one obtains an *approximation* to the exact RG trajectory projected onto the chosen subspace. Note that this approximate trajectory does, in general, not coincide with the projection of the exact trajectory, but if the subspace is well chosen, it will not be very different from it.

8.3 The Effective Average Action for Gravity

The effective average action for gravity which has been introduced in ref. [11] is a concrete implementation of the general ideas outlined above. The ultimate goal is to give meaning to an integral over 'all' metrics $\gamma_{\mu\nu}$ of the form $\int\mathscr{D}\gamma_{\mu\nu}\exp\{-S[\gamma_{\mu\nu}] + \text{source terms}\}$ whose bare action $S[\gamma_{\mu\nu}]$ is invariant under general coordinate transformations. The first step consists in splitting the quantum metric according to

$$\gamma_{\mu\nu} = \overline{\mathrm{g}}_{\mu\nu} + h_{\mu\nu} \tag{8.12}$$

where $\overline{\mathrm{g}}_{\mu\nu}$ is a fixed, but unspecified, background metric and $h_{\mu\nu}$ are the quantum fluctuations around this background which are not necessarily small. This allows

the formal construction of the gauge-fixed (Euclidean) gravitational path integral

$$\int \mathscr{D}h\mathscr{D}C^{\mu}\mathscr{D}\bar{C}_{\mu}\exp\bigl\{-S[\overline{\mathrm{g}}+h]-S^{\mathrm{gf}}[h;\overline{\mathrm{g}}]-S^{\mathrm{ghost}}[h,C,\bar{C};\overline{\mathrm{g}}]-\Delta_k S[h,C,\bar{C};\overline{\mathrm{g}}]\bigr\}. \tag{8.13}$$

Here $S[\overline{\mathrm{g}}+h]$ is a generic action, which depends on $\gamma_{\mu\nu}$ only, while the background gauge fixing $S^{\mathrm{gf}}[h;\overline{\mathrm{g}}]$ and ghost contribution $S^{\mathrm{ghost}}[h,C,\bar{C};\overline{\mathrm{g}}]$ contain $\overline{\mathrm{g}}_{\mu\nu}$ and $h_{\mu\nu}$ in such a way that they do not combine into a full $\gamma_{\mu\nu}$. We take $S^{\mathrm{gf}}[h;\overline{\mathrm{g}}]$ to be a gauge fixing 'of the background type' [141], i.e., it is invariant under diffeomorphisms acting on both $h_{\mu\nu}$ and $\bar{g}_{\mu\nu}$.

The key ingredient in the construction of the FRGE is the coarse graining term $\Delta_k S[h,C,\bar{C};\overline{\mathrm{g}}]$. It is quadratic in the fluctuation field,

$$\int d^dx\sqrt{\overline{\mathrm{g}}}h_{\mu\nu}\mathscr{R}_k^{\mu\nu\rho\sigma}\bigl(-\bar{D}^2\bigr)h_{\rho\sigma},$$

plus a similar term for the ghosts. The kernel $\mathscr{R}_k^{\mu\nu\rho\sigma}(p^2)$ provides a k-dependent mass term which separates the fluctuations into high momentum modes $p^2\gg k^2$ and low momentum modes $p^2\ll k^2$ with respect to the scale set by the covariant Laplacian of the background metric. The profile of $\mathscr{R}_k^{\mu\nu\rho\sigma}(p^2)$ ensures that the high momentum modes are integrated out unsuppressed while the contribution of the low momentum modes to the path integral is suppressed by the k-dependent mass term. Varying k then naturally realizes Wilson's idea of coarse graining by integrating out the quantum fluctuations shell by shell.

The k-derivative of Eq. (8.13) with $h_{\mu\nu}$ and the ghosts coupled to appropriate sources, provides the starting point for the construction of the functional renormalization group equation for the effective average action Γ_k [61–67]. (See [68, 69] for reviews.) For gravity this flow equation takes the form [11]

$$\partial_t\Gamma_k[\bar{h},\xi,\bar{\xi};\overline{\mathrm{g}}]=\frac{1}{2}\mathrm{STr}\bigl[\bigl(\Gamma_k^{(2)}+\mathscr{R}_k\bigr)^{-1}\partial_t\mathscr{R}_k\bigr]. \tag{8.14}$$

Here $t=\log(k/k_0)$, STr is a functional supertrace which includes a minus sign for the ghosts $\xi\equiv\langle C\rangle$, $\bar{\xi}\equiv\langle\bar{C}\rangle$, $\mathscr{R}_k$ is the matrix-valued (in field space) IR cutoff introduced above, and $\Gamma_k^{(2)}$ is the second variation of Γ_k with respect to the *fluctuation fields*. Notably, $\Gamma_k[\bar{h},\xi,\bar{\xi};\overline{\mathrm{g}}]$ depends on *two* metrics, $\overline{\mathrm{g}}_{\mu\nu}$ and

$$g_{\alpha\beta}\equiv\langle\gamma_{\alpha\beta}\rangle=\overline{\mathrm{g}}_{\alpha\beta}+\bar{h}_{\alpha\beta},\qquad \bar{h}_{\alpha\beta}\equiv\langle h_{\alpha\beta}\rangle. \tag{8.15}$$

In this sense, Γ_k is of an intrinsically *bimetric* nature, and therefore we often write $\Gamma_k[g,\overline{\mathrm{g}},\xi,\bar{\xi}]\equiv\Gamma_k[\bar{h}=g-\overline{\mathrm{g}},\xi,\bar{\xi};\overline{\mathrm{g}}]$. This functional is invariant under background gauge transformations acting on all four fields simultaneously. It is a k-dependent generalization of the standard effective action $\Gamma\equiv\Gamma_0$ to which it reduces in the limit $k\to 0$. It can also be shown that Γ_k in the limit $k\to\infty$ is essentially equivalent to the bare action S. (For further details about Γ_k for gravity we refer to [11].)

8.4 The Einstein–Hilbert Truncation

Solving the FRGE (8.14) is equivalent to (and as difficult as) calculating the functional integral over $\gamma_{\mu\nu}$. It is therefore important to devise efficient approximation methods. The truncation of theory space is the one which makes maximum use of the FRGE reformulation of the quantum field theory problem at hand.

The first truncation for which the RG flow has been worked out [11] is the 'Einstein–Hilbert truncation' which retains in Γ_k only the terms $\int d^dx\sqrt{g}$ and $\int d^dx\sqrt{g}R$, already present in the in the classical action, with k-dependent coupling constants, as well as the classical gauge fixing and ghost terms:

$$\Gamma_k = \frac{1}{16\pi G_k}\int d^dx\sqrt{g}\{-R+2\bar{\lambda}_k\} + \text{class. gf- and gh-terms.} \tag{8.16}$$

In this case the truncation subspace is 2-dimensional. The ansatz (8.16) contains two free functions of the scale, the running cosmological constant $\bar{\lambda}_k$ and the running Newton constant G_k.

Upon inserting the ansatz (8.16) into the flow equation (8.14) it boils down to a system of two ordinary differential equations. We shall display them here in terms of the dimensionless running cosmological constant and Newton constant, respectively:

$$\lambda_k \equiv k^{-2}\bar{\lambda}_k, \qquad g_k \equiv k^{d-2}G_k. \tag{8.17}$$

Using λ_k and g_k the RG equations become autonomous

$$k\partial_k g(k) = \beta_g\big[g(k),\lambda(k)\big], \qquad k\partial_k\lambda(k) = \beta_\lambda\big[g(k),\lambda(k)\big], \tag{8.18}$$

with

$$\beta_g(g_k,\lambda_k) = \big[d-2+\eta_N(g_k,\lambda_k)\big]g_k. \tag{8.19}$$

Here $\eta_N \equiv \partial_t \ln G_k$ is the anomalous dimension of the operator $\sqrt{g}R$. The explicit form of the beta functions β_g and β_λ for arbitrary cutoff $\mathscr{R}_k$ and dimension can be found in ref. [11]. Here we only display the result for $d=4$ and a sharp cutoff:

$$\partial_t\lambda_k = -(2-\eta_N)\lambda_k - \frac{g_k}{\pi}\left[5\ln(1-2\lambda_k) - 2\zeta(3) + \frac{5}{2}\eta_N\right], \tag{8.20a}$$

$$\partial_t g_k = (2+\eta_N)g_k, \tag{8.20b}$$

$$\eta_N = -\frac{2g_k}{6\pi+5g_k}\left[\frac{18}{1-2\lambda_k} + 5\ln(1-2\lambda_k) - \zeta(2) + 6\right]. \tag{8.20c}$$

In [14] this system has been analyzed in detail, using both analytical and numerical methods. In particular all RG trajectories have been classified, and examples have been computed numerically. The most important classes of trajectories in the phase portrait on the g–λ-plane are shown in Fig. 8.2.

The RG flow is found to be dominated by two fixed points (g^*,λ^*): the GFP at $g^*=\lambda^*=0$, and a NGFP with $g^*>0$ and $\lambda^*>0$. There are three classes of

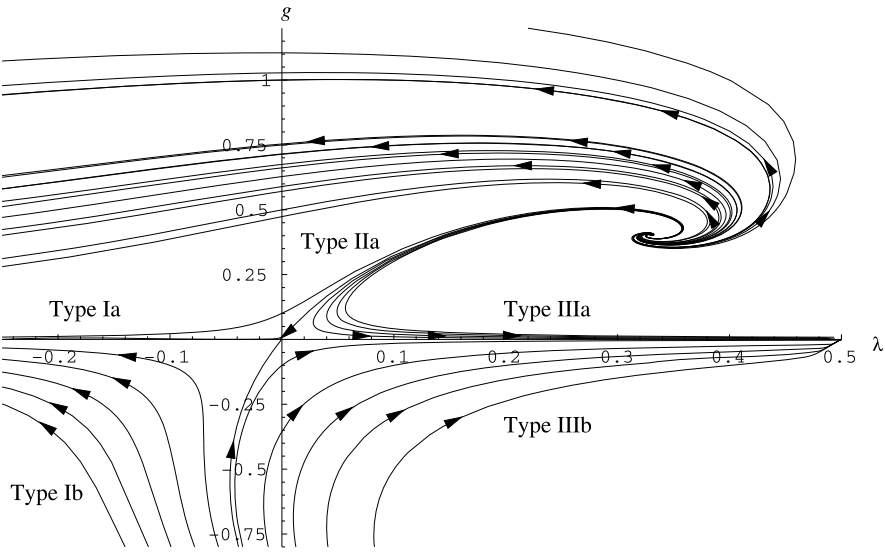

Fig. 8.2 RG flow in the g–λ-plane. The arrows point in the direction of increasing coarse graining, i.e., of decreasing k. (From [14])

trajectories emanating from the NGFP: trajectories of Type Ia and IIIa run towards negative and positive cosmological constants, respectively, and the single trajectory of Type IIa ('separatrix') hits the GFP for $k \to 0$. The high momentum properties of QEG are governed by the NGFP; for $k \to \infty$, in Fig. 8.2 all RG trajectories on the half-plane $g > 0$ run into this point. The two critical exponents are a complex conjugate pair $\theta_{1,2} = \theta' \pm i\theta''$ with $\theta' > 0$. The fact that at the NGFP the dimensionless coupling constants g_k, λ_k approach constant, non-zero values then implies that the dimensionful quantities run according to

$$G_k = g^* k^{2-d}, \qquad \bar{\lambda}_k = \lambda^* k^2. \tag{8.21}$$

Hence for $k \to \infty$ and $d > 2$ the dimensionful Newton constant vanishes while the cosmological constant diverges.

So, the Einstein–Hilbert truncation does indeed predict the existence of a NGFP with exactly the properties needed for the asymptotic safety construction. Clearly the crucial question is whether the NGFP found is the projection of an exact fixed point in the full theory or merely the artifact of an insufficient approximation. This question has been analyzed during the past decade within truncations of ever increasing complexity. All investigations performed to date support the existence of a NGFP in the exact theory, and without exception they predict a projected RG flow on the g–λ-plane which is qualitatively similar to that of the Einstein–Hilbert truncation. In fact, the phase portrait in Fig. 8.2 has survived substantial generalizations of the truncation ansatz for the average action. Furthermore, clear evidence for a small, finite dimensionality of $\mathscr{S}_{\rm UV}$ was found, first in $2 + \varepsilon$ dimensions [15] and then by an impressively complex calculation in $d = 4$ also [31, 32].

Beside its successes in describing gravity at high energies, QEG also recovers classical general relativity at low energies. Concretely, it was shown in [123–125] that Fig. 8.2 contains Type IIIa trajectories which are in agreement with observational data. This analysis is fairly robust and clear-cut; it does not involve the NGFP. All that is needed is the RG flow linearized about the GFP. In its vicinity one has [11]

$$\bar{\lambda}(k) = \bar{\lambda}_0 + \nu \bar{G} k^d + \cdots, \qquad G(k) = \bar{G} + \cdots, \tag{8.22}$$

i.e., $\bar{\lambda}$ displays a running $\propto k^d$ and G is approximately constant. Here ν is a positive constant of order unity [11, 14]. These equations are valid if $\lambda(k) \ll 1$ and $g(k) \ll 1$. They describe a 2-parameter family of RG trajectories labeled by the pair $(\bar{\lambda}_0, \bar{G})$. It will prove convenient to use an alternative labeling $(\lambda_\mathrm{T}, k_\mathrm{T})$ with $\lambda_\mathrm{T} \equiv (4\nu\bar{\lambda}_0\bar{G})^{1/2}$ and $k_\mathrm{T} \equiv (\bar{\lambda}_0/\nu\bar{G})^{1/4}$. The old labels are expressed in terms of the new ones as $\bar{\lambda}_0 = \frac{1}{2}\lambda_\mathrm{T} k_\mathrm{T}^2$ and $\bar{G} = \lambda_\mathrm{T}/(2\nu k_\mathrm{T}^2)$. It is furthermore convenient to introduce the abbreviation $g_\mathrm{T} \equiv \lambda_\mathrm{T}/(2\nu)$. When parameterized by the pair $(\lambda_\mathrm{T}, k_\mathrm{T})$ the trajectories assume the form

$$\begin{aligned} \bar{\lambda}(k) &= \frac{1}{2}\lambda_\mathrm{T} k_\mathrm{T}^2 \big[1 + (k/k_\mathrm{T})^4\big] \equiv \bar{\lambda}_0 \big[1 + (k/k_\mathrm{T})^4\big], \\ G(k) &= \frac{\lambda_\mathrm{T}}{2\nu k_\mathrm{T}^2} \equiv \frac{g_\mathrm{T}}{k_\mathrm{T}^2}, \end{aligned} \tag{8.23}$$

or, in dimensionless form,

$$\lambda(k) = \frac{1}{2}\lambda_\mathrm{T}\left[\left(\frac{k_\mathrm{T}}{k}\right)^2 + \left(\frac{k}{k_\mathrm{T}}\right)^2\right], \qquad g(k) = g_\mathrm{T}\left(\frac{k}{k_\mathrm{T}}\right)^2. \tag{8.24}$$

As for the interpretation of the new variables, it is clear that $\lambda_\mathrm{T} \equiv \lambda(k \equiv k_\mathrm{T})$ and $g_\mathrm{T} \equiv g(k = k_\mathrm{T})$, while k_T is the scale at which β_λ (but not β_g) vanishes according to the linearized running: $\beta_\lambda(k_\mathrm{T}) \equiv k d\lambda(k)/dk|_{k=k_\mathrm{T}} = 0$. Thus we see that $(g_\mathrm{T}, \lambda_\mathrm{T})$ are the coordinates of the turning point T of the Type IIIa trajectory considered, and k_T is the scale at which it is passed. The regimes $k > k_\mathrm{T}$ ($k < k_\mathrm{T}$) are conveniently referred to as the 'UV regime' ('IR regime').

Let us now hypothesize that, within a certain range of k-values, the RG trajectory realized in Nature can be approximated by (8.24). In order to determine its parameters $(\bar{\lambda}_0, \bar{G})$ or $(\lambda_\mathrm{T}, k_\mathrm{T})$ we must perform a measurement of G and $\bar{\lambda}$. If we interpret the observed values $G_\mathrm{observed} = m_\mathrm{Pl}^{-2}$, $m_\mathrm{Pl} \approx 1.2 \times 10^{19}$ GeV, and $\bar{\lambda}_\mathrm{observed} \approx 10^{-120} m_\mathrm{Pl}^2$ as the running $G(k)$ and $\bar{\lambda}(k)$ evaluated at a scale $k \ll k_\mathrm{T}$, then we get from (8.23) that $\bar{\lambda}_0 = \bar{\lambda}_\mathrm{observed}$ and $\bar{G} = G_\mathrm{observed}$. Using the definitions of λ_T and k_T along with $\nu = O(1)$ this leads to the order-of-magnitude estimates $g_\mathrm{T} \approx \lambda_\mathrm{T} \approx 10^{-60}$ and $k_\mathrm{T} \approx 10^{-30} m_\mathrm{Pl} \approx (10^{-3}\ \mathrm{cm})^{-1}$. Because of the tiny values of g_T and λ_T the turning point lies in the linear regime of the GFP. Going beyond the linear regime, the k-dependence of G and $\bar{\lambda}$ is plotted schematically in Fig. 8.3.

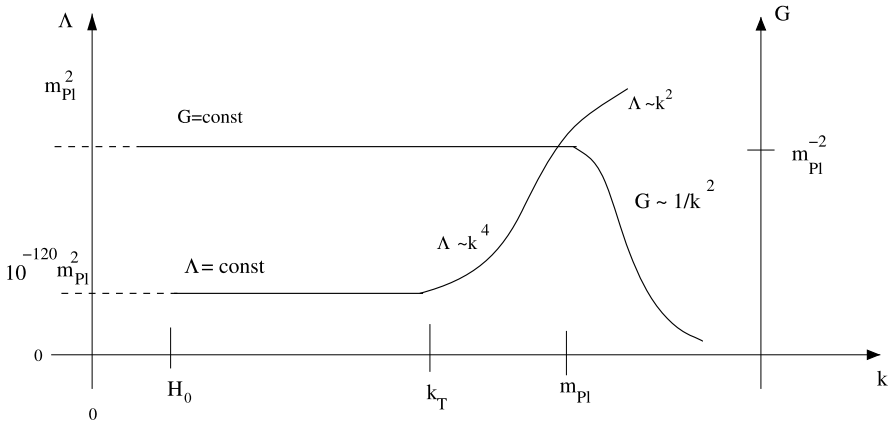

Fig. 8.3 The dimensionful $\Lambda(k) \equiv \bar{\lambda}(k)$ and $G(k)$ for a Type IIIa trajectory with realistic parameters

8.5 The Multi-fractal Properties of QEG Space-Times

We now proceed by discussing an intriguing consequence arising from the scale-dependence of the gravitational effective action, namely that the QEG space-time at short distances develops fractal properties [13, 15, 97]. As we have seen, the effective average action $\Gamma_k[g_{\mu\nu}]$ defines an infinite set of effective field theories, valid near a variable mass scale k. Intuitively speaking, the solution $\langle g_{\mu\nu}\rangle_k$ of the scale dependent field equation

$$\frac{\delta \Gamma_k}{\delta g_{\mu\nu}(x)}\big[\langle g\rangle_k\big] = 0 \tag{8.25}$$

can be interpreted as the metric averaged over (Euclidean) space-time volumes of a linear extension ℓ which typically is of the order of $1/k$. Knowing the scale dependence of Γ_k, i.e., the renormalization group trajectory $k \mapsto \Gamma_k$, we can in principle follow the solution $\langle g_{\mu\nu}\rangle_k$ from the ultraviolet ($k \to \infty$) to the infrared ($k \to 0$).

(1) Quantum space-times. It is an important feature of this approach that the infinitely many equations of (8.25), one for each scale k, are valid *simultaneously*. They all refer *to the same* physical system, the 'quantum space-time', but describe its effective metric structure on different scales. An observer using a 'microscope' with a resolving power $\ell \approx k^{-1}$ will perceive the Universe to be a Riemannian manifold with metric $\langle g_{\mu\nu}\rangle_k$.[1] At every fixed k, $\langle g_{\mu\nu}\rangle_k$ is a smooth classical metric. But since the quantum space-time is characterized by the infinity of Eqs. (8.25) with $k = 0, \ldots, \infty$ it can acquire very non-classical and in particular fractal features. In

[1]The 'resolving power' ℓ of the microscope is in general a complicated function of k. It can be found by an algorithm outlined in [97]. For the purposes of the present discussion it is sufficient to think of this relationship as $\ell \approx 1/k$, like on flat space.

particular, it was concluded in [13, 15] that the effective dimensionality of space-time is scale dependent. It equals 4 at macroscopic distances ($\ell \gg \ell_{\rm Pl}$) but, near $\ell \approx \ell_{\rm Pl}$, it gets dynamically reduced to the value 2. For $\ell \ll \ell_{\rm Pl}$ space-time resembles a 2-dimensional fractal. In the following we review the arguments that led to this conclusion.

(2) Self-similarity in the fixed point regime. For simplicity we use the Einstein–Hilbert truncation to start with, and we consider space-times with classical dimensionality $d = 4$. The corresponding RG trajectories are shown in Fig. 8.2. The physically relevant ones, for $k \to \infty$, all approach the NGFP at (g_*, λ_*) so that the dimensionful quantities run according to (8.21). This scaling behavior is realized in the asymptotic scaling regime $k \gg m_{\rm Pl}$. Near $k = m_{\rm Pl}$ the trajectories cross over towards the GFP at $g = \lambda = 0$, and then run towards negative, vanishing, and positive values of λ, respectively. For our present purpose, it suffices to consider the limiting cases of very small and very large distances of a RG trajectory. We assume that G_k and $\bar{\lambda}_k$ behave as in (8.21) for $k \gg m_{\rm Pl}$, and that they are constant for $k \ll m_{\rm Pl}$. The precise interpolation between the two regimes will not be needed here.

The argument of ref. [15] concerning the fractal nature of the QEG space-times was as follows. Within the Einstein–Hilbert truncation of theory space, the effective field equations (8.25) happen to coincide with the ordinary Einstein equation, but with G_k and $\bar{\lambda}_k$ replacing the classical constants. Without matter,

$$R_{\mu\nu}\big(\langle g\rangle_k\big) = \frac{2}{2-d}\bar{\lambda}_k \langle g_{\mu\nu}\rangle_k . \tag{8.26}$$

Since in absence of dimensionful constants of integration $\bar{\lambda}_k$ is the only quantity in this equation which sets a scale, every solution to (8.26) has a typical radius of curvature $r_c(k) \propto 1/\sqrt{\bar{\lambda}_k}$. (For instance, the maximally symmetric S^4-solution has the radius $r_c = r = \sqrt{3/\bar{\lambda}_k}$.) If we want to explore the space-time structure at a fixed length scale ℓ we should use the action $\Gamma_k[g_{\mu\nu}]$ at $k = 1/\ell$ because with this functional a tree level analysis is sufficient to describe the essential physics at this scale, including the relevant quantum effects. Hence, when we observe the space-time with a microscope of resolution ℓ, we will see an average radius of curvature given by $r_c(\ell) \equiv r_c(k = 1/\ell)$. Once ℓ is smaller than the Planck length $\ell_{\rm Pl} \equiv m_{\rm Pl}^{-1}$ we are in the fixed point regime where $\bar{\lambda}_k \propto k^2$ so that $r_c(k) \propto 1/k$, or

$$\boxed{r_c(\ell) \propto \ell .} \tag{8.27}$$

Thus, when we look at the structure of space-time with a microscope of resolution $\ell \ll \ell_{\rm Pl}$, the average radius of curvature which we measure is proportional to the resolution itself. If we want to probe finer details and decrease ℓ we automatically decrease r_c and hence *in*crease the average curvature. Space-time seems to be more strongly curved at small distances than at larger ones. The scale-free relation (8.27) suggests that at distances below the Planck length the QEG space-time is a special kind of fractal with a self-similar structure. It has no intrinsic scale because in the fractal regime, i.e., when the RG trajectory is still close to the NGFP, the parameters

which usually set the scales of the gravitational interaction, G and $\bar{\lambda}$, are not yet 'frozen out'. This happens only later on, somewhere half way between the non-Gaussian and the Gaussian fixed point, at a scale of the order of $m_{\rm Pl}$.

Below this scale, G_k and $\bar{\lambda}_k$ stop running and, as a result, $r_c(k)$ becomes independent of k so that $r_c(\ell) = \text{const}$ for $\ell \gg \ell_{\rm Pl}$. In this regime $\langle g_{\mu\nu}\rangle_k$ is k-independent, indicating that the macroscopic space-time is describable by a single smooth, classical Riemannian manifold.

(3) Anomalous dimension and graviton propagator. An independent argument supporting the assertion that the QEG space-time has an effective dimensionality which is k-dependent and non-integer in general based upon the *anomalous dimension* $\eta_N \equiv \partial_t \ln G_k$ has been put forward in ref. [13]. In a sense which we shall make more precise in a moment, the effective dimensionality of space-time equals $4 + \eta_N$. The RG trajectories of the Einstein–Hilbert truncation (within its domain of validity) have $\eta_N \approx 0$ for $k \to 0$ and $\eta_N \approx -2$ for $k \to \infty$, the smooth change by two units occurring near $k \approx m_{\rm Pl}$. As a consequence, the effective dimensionality is 4 for $\ell \gg \ell_{\rm Pl}$ and 2 for $\ell \ll \ell_{\rm Pl}$.

In fact, the UV fixed point has an anomalous dimension $\eta \equiv \eta_N(g_*, \lambda_*) = -2$. We can use this information in order to determine the momentum dependence of the dressed graviton propagator for momenta $p^2 \gg m_{\rm Pl}^2$. Expanding (8.16) about flat space and omitting the standard tensor structures we find the inverse propagator $\widetilde{\mathscr{G}}_k(p)^{-1} \propto G_k^{-1} p^2$. The conventional dressed propagator $\widetilde{\mathscr{G}}(p)$ contained in $\Gamma \equiv \Gamma_{k=0}$ is obtained from the *exact* $\widetilde{\mathscr{G}}_k$ in the limit $k \to 0$. For $p^2 > k^2 \gg m_{\rm Pl}^2$ the actual cutoff scale is the physical momentum p^2 itself so that the k-evolution of $\widetilde{\mathscr{G}}_k(p)$ stops at the threshold $k = \sqrt{p^2}$. Therefore,

$$\widetilde{\mathscr{G}}(p)^{-1} \propto p^2 G_k^{-1}\big|_{k=\sqrt{p^2}} \propto \left(p^2\right)^{1-\frac{\eta}{2}} \tag{8.28}$$

because $G_k^{-1} \propto k^{-\eta}$ when η is (approximately) constant. In d flat dimensions, and for $\eta \neq 2 - d$, the Fourier transform of $\widetilde{\mathscr{G}}(p) \propto 1/(p^2)^{1-\eta/2}$ yields the following propagator in position space:

$$\mathscr{G}(x; y) \propto \frac{1}{|x - y|^{d-2+\eta}}. \tag{8.29}$$

This form of the propagator is well known from the theory of critical phenomena, for instance. (In the latter case it applies to large distances.) Equation (8.29) is not valid directly at the NGFP. For $d = 4$ and $\eta = -2$ the dressed propagator is $\widetilde{\mathscr{G}}(p) = 1/p^4$, which has the following representation in position space:

$$\mathscr{G}(x; y) = -\frac{1}{8\pi^2} \ln\big(\mu|x - y|\big). \tag{8.30}$$

Here μ is an arbitrary constant with the dimension of a mass. Obviously (8.30) has the same form as a $1/p^2$-propagator in 2 dimensions.

Slightly away from the NGFP, before other physical scales intervene, the propagator is of the familiar type (8.29) which shows that the quantity η_N has the standard interpretation of an anomalous dimension in the sense that fluctuation effects modify the decay properties of $\mathscr{G}$ so as to correspond to a space-time of effective dimensionality $4+\eta_N$.

Thus the properties of the RG trajectories imply a remarkable dimensional reduction: *Space-time, probed by a 'graviton' with $p^2 \ll m_{\rm Pl}^2$ is 4-dimensional, but it appears to be 2-dimensional for a graviton with $p^2 \gg m_{\rm Pl}^2$* [13]. More generally, in d classical dimensions, where the macroscopic space-time is d-dimensional, the anomalous dimension at the fixed point is $\eta_N = 2-d$. Therefore, for any d, the dimensionality of the fractal as implied by η_N is $d+\eta_N = 2$ [13, 15].

8.6 Spectral, Walk, and Hausdorff Dimension

The fractal properties of the QEG space-time can be further quantified by investigating random walks and diffusion processes on fractals. In this course one is led to introduce various notions of fractal dimensions, such as the spectral or walk dimension [142]. A priori they have no reason to equal the effective dimension $d_{\rm eff} = d+\eta$ implied by the running Newton constant and the graviton propagator.

(1) The spectral dimension. Consider the diffusion process where a spinless test particle performs a Brownian random walk on an ordinary Riemannian manifold with a fixed classical metric $g_{\mu\nu}(x)$. It is described by the heat-kernel $K_g(x,x';T)$ which gives the probability density for a transition of the particle from x to x' during the fictitious time T. It satisfies the heat equation

$$\partial_T K_g\big(x,x';T\big) = -\Delta_g K_g\big(x,x';T\big), \tag{8.31}$$

where $\Delta_g = -D^2$ denotes the Laplace operator. In flat space, this equation is easily solved by

$$K_g\big(x,x';T\big) = \int \frac{d^d p}{(2\pi)^d} e^{ip\cdot(x-x')} e^{-p^2 T}. \tag{8.32}$$

In general, the heat-kernel is a matrix element of the operator $\exp(-T\Delta_g)$. In the random walk picture its trace per unit volume,

$$P_g(T) = V^{-1}\int d^d x\sqrt{g(x)}K_g(x,x;T) \equiv V^{-1}\,{\rm Tr}\exp(-T\Delta_g), \tag{8.33}$$

has the interpretation of an average return probability. Here $V \equiv \int d^d x\sqrt{g(x)}$ denotes the total volume. It is well known that P_g possesses an asymptotic early time expansion (for $T\to 0$) of the form $P_g(T) = (4\pi T)^{-d/2}\sum_{n=0}^{\infty} A_n T^n$, with A_n denoting the Seeley–DeWitt coefficients. From this expansion one can motivate the

definition of the spectral dimension d_s as the T-independent logarithmic derivative

$$d_s \equiv -2 \frac{d \ln P_g(T)}{d \ln T}\bigg|_{T=0}. \tag{8.34}$$

On smooth manifolds, where the early-time expansion of $P_g(T)$ is valid, the spectral dimension agrees with the topological dimension d of the manifold.

Given $P_g(T)$, it is natural to define an, in general T-dependent, generalization of the spectral dimension by

$$\mathscr{D}_s(T) \equiv -2 \frac{d \ln P_g(T)}{d \ln T}. \tag{8.35}$$

According to (8.34), we recover the true spectral dimension of the space-time by considering the shortest possible random walks, i.e., by taking the limit $d_s = \lim_{T \to 0} \mathscr{D}_s(T)$. Note that in view of a possible comparison with other (discrete) approaches to quantum gravity the generalized, scale-dependent version (8.35) will play a central role later on.

(2) The walk dimension. Regular Brownian motion in flat space has the celebrated property that the random walker's average square displacement increases linearly with time: $\langle r^2 \rangle \propto T$. Indeed, performing the integral (8.32) we obtain the familiar probability density

$$K\left(x, x'; T\right) = \frac{1}{(4\pi T)^{d/2}} \exp\left(-\frac{|x - x'|^2}{4T}\right). \tag{8.36}$$

Using (8.36) yields the expectation value $\langle r^2 \rangle \equiv \langle x^2 \rangle = \int d^d x \, x^2 K(x, 0; T) \propto T$.

Many diffusion processes of physical interest (such as diffusion on fractals) are anomalous in the sense that this linear relationship is generalized to a power law $\langle r^2 \rangle \propto T^{2/d_w}$ with $d_w \neq 2$. The interpretation of the so-called walk dimension d_w is as follows. The trail left by the random walker is a random object, which is interesting in its own right. It has the properties of a fractal, even in the 'classical' case when the walk takes place on a regular manifold. The quantity d_w is precisely the fractal dimension of this trail. Diffusion processes are called regular if $d_w = 2$, and anomalous when $d_w \neq 2$.

(3) The Hausdorff dimension. Finally, we introduce the Hausdorff dimension d_H. Instead of working with its mathematically rigorous definition in terms of the Hausdorff measure and all possible covers of the metric space under consideration, the present, simplified definition may suffice for our present purposes. On a smooth set, the scaling law for the volume $V(r)$ of a d-dimensional ball of radius r takes the form

$$V(r) \propto r^{d_H}. \tag{8.37}$$

The Hausdorff dimension is then obtained in the limit of infinitely small radius,

$$d_H \equiv \lim_{r \to 0} \frac{\ln V(r)}{\ln r}. \tag{8.38}$$

Contrary to the spectral or walk dimension whose definitions are linked to dynamical diffusion processes on space-time, no such dynamics is associated with d_H.

8.7 Fractal Dimensions Within QEG

Upon introducing various concepts for fractal dimensions in the last section, we now proceed with their evaluation for the QEG effective space-times, following refs. [97] and [99]. Our discussion will mostly be based on the Einstein–Hilbert truncation. As we shall see this restriction is actually unnecessary in the asymptotic scaling regime, i.e., when the RG trajectory is close to the NGFP. In this case we can derive *exact* results for the spectral and walk dimension by exploiting the scale invariance of the theory at the fixed point.

8.7.1 Diffusion Processes on QEG Space-Times

Since in QEG one integrates over all metrics, the central idea is to replace $P_g(T)$ by its expectation value

$$P(T) \equiv \big\langle P_\gamma(T) \big\rangle \equiv \int \mathscr{D}\gamma \mathscr{D}C \mathscr{D}\bar{C}\, P_\gamma(T) \exp\big(-S_{\rm bare}[\gamma, C, \bar{C}]\big). \tag{8.39}$$

Here $\gamma_{\mu\nu}$ denotes the microscopic metric and $S_{\rm bare}$ is the bare action related to the UV fixed point, with the gauge-fixing and the pieces containing the ghosts C and $\bar{C}$ included. For the untraced heat-kernel, we define likewise $K(x, x'; T) \equiv \langle K_\gamma(x, x'; T)\rangle$. These expectation values are most conveniently calculated from the effective average action Γ_k, which equips the d-dimensional smooth manifolds underlying the QEG effective space-times with a family of metric structures $\{\langle g_{\mu\nu}\rangle_k, 0 \le k < \infty\}$, one for each coarse-graining scale k [82, 97]. These metrics are solutions to the effective field equations implied by Γ_k.

We shall again approximate the latter by the Einstein–Hilbert truncation (8.16). The corresponding effective field equation is given by (8.26). Based on this equation, we can easily find the k-dependence of the corresponding solution $\langle g_{\mu\nu}\rangle_k$ by rewriting (8.26) as $[\bar{\lambda}_{k_0}/\bar{\lambda}_k] R^\mu{}_\nu(\langle g\rangle_k) = \frac{2}{2-d}\bar{\lambda}_{k_0}\delta^\mu{}_\nu$ for some fixed reference scale k_0, and exploiting that $R^\mu{}_\nu(cg) = c^{-1}R^\mu{}_\nu(g)$ for any constant $c > 0$. This shows that the metric and its inverse scale according to, for any d,

$$\big\langle g_{\mu\nu}(x)\big\rangle_k = \frac{\bar{\lambda}_{k_0}}{\bar{\lambda}_k}\big\langle g_{\mu\nu}(x)\big\rangle_{k_0}, \qquad \big\langle g^{\mu\nu}(x)\big\rangle_k = \frac{\bar{\lambda}_k}{\bar{\lambda}_{k_0}}\big\langle g^{\mu\nu}(x)\big\rangle_{k_0}. \tag{8.40}$$

Denoting the Laplace operators corresponding to the metrics $\langle g_{\mu\nu}\rangle_k$ and $\langle g_{\mu\nu}\rangle_{k_0}$ by $\Delta(k)$ and $\Delta(k_0)$, respectively, these relations imply

$$\Delta(k) = \frac{\bar{\lambda}_k}{\bar{\lambda}_{k_0}}\Delta(k_0). \tag{8.41}$$

At this stage, the following remark is in order. In the asymptotic scaling regime associated with the NGFP, the scale-dependence of the couplings is fixed by the fixed-point condition (8.21). This implies in particular

$$\langle g_{\mu\nu}(x)\rangle_k \propto k^{-2} \quad (k \to \infty). \tag{8.42}$$

This asymptotic relation is actually an *exact* consequence of asymptotic safety, which solely relies on the scale-independence of the theory at the fixed point.

We can evaluate the expectation value (8.39) by exploiting the effective field theory properties of the effective average action. Since Γ_k defines an effective field theory at the scale k we know that $\langle \mathcal{O}(\gamma_{\mu\nu})\rangle \approx \mathcal{O}(\langle g_{\mu\nu}\rangle_k)$ provided the observable $\mathcal{O}$ involves only momentum scales of the order of k. We apply this rule to the RHS of the diffusion equation, $\mathcal{O} = -\Delta_\gamma K_\gamma(x, x'; T)$. The subtle issue here is the correct identification of k. If the diffusion process involves (approximately) only a small interval of scales near k over which $\bar{\lambda}_k$ does not change much, the corresponding heat equation contains the operator $\Delta(k)$ for this specific, fixed value of k: $\partial_T K(x, x'; T) = -\Delta(k) K(x, x'; T)$. Denoting the eigenvalues of $\Delta(k_0)$ by $\mathcal{E}_n$ and the corresponding eigenfunctions by ϕ_n, this equation is solved by

$$K\big(x, x'; T\big) = \sum_n \phi_n(x)\phi_n\big(x'\big) \exp\big[-F\big(k^2\big)\mathcal{E}_n T\big]. \tag{8.43}$$

Here we introduced the convenient notation $F(k^2) \equiv \bar{\lambda}_k/\bar{\lambda}_{k_0}$. Knowing the propagation kernel, we can time-evolve any initial probability distribution $p(x; 0)$ according to

$$p(x; T) = \int d^d x' \sqrt{g_0\big(x'\big)}\, K\big(x, x'; T\big)\, p\big(x'; 0\big), \tag{8.44}$$

with g_0 the determinant of $\langle g_{\mu\nu}\rangle_{k_0}$. If the initial distribution has an eigenfunction expansion of the form $p(x; 0) = \sum_n C_n \phi_n(x)$, we obtain

$$p(x; T) = \sum_n C_n \phi_n(x) \exp\big[-F\big(k^2\big)\mathcal{E}_n T\big]. \tag{8.45}$$

If the C_n's are significantly different from zero only for a single eigenvalue $\mathcal{E}_N$, we are dealing with a single-scale problem and would identify $k^2 = \mathcal{E}_N$ as the relevant scale at which the running couplings are to be evaluated. In general the C_n's are different from zero over a wide range of eigenvalues. In this case we face a multiscale problem where different modes ϕ_n probe the space-time on different length scales. If $\Delta(k_0)$ corresponds to flat space, say, the eigenfunctions $\phi_n = \phi_p$ are plane waves with momentum p^μ, and they resolve structures on a length scale ℓ of order $1/|p|$. Hence, in terms of the eigenvalue $\mathcal{E}_n \equiv \mathcal{E}_p = p^2$ the resolution is $\ell \approx 1/\sqrt{\mathcal{E}_n}$. This suggests that when the manifold is probed by a mode with eigenvalue $\mathcal{E}_n$ it 'sees' the metric $\langle g_{\mu\nu}\rangle_k$ for the scale $k = \sqrt{\mathcal{E}_n}$. Actually, the identification $k = \sqrt{\mathcal{E}_n}$ is correct also for curved space since, in the construction of Γ_k, the parameter k is introduced precisely as a cutoff in the spectrum of the covariant Laplacian.

As a consequence, under the spectral sum of (8.45), we must use the scale $k^2 = \mathscr{E}_n$ which depends explicitly on the resolving power of the corresponding mode. Likewise, in Eq. (8.43), $F(k^2)$ is to be interpreted as $F(\mathscr{E}_n)$:

$$K(x,x';T) = \sum_n \phi_n(x)\phi_n(x') \exp\bigl[-F(\mathscr{E}_n)\mathscr{E}_n T\bigr]$$
$$= \sum_n \phi_n(x) \exp\bigl\{-F\bigl[\Delta(k_0)\bigr]\Delta(k_0)T\bigr\}\phi_n(x'). \tag{8.46}$$

As in [97], we choose k_0 as a macroscopic scale in the classical regime, and we assume that at k_0 the cosmological constant is small, so that $\langle g_{\mu\nu}\rangle_{k_0}$ can be approximated by the flat metric on $\mathbb{R}^d$. The eigenfunctions of $\Delta(k_0)$ are plane waves then and Eq. (8.46) becomes

$$K(x,x';T) = \int \frac{d^d p}{(2\pi)^d} e^{ip\cdot(x-x')} e^{-p^2 F(p^2)T}, \tag{8.47}$$

where the scalar products are performed with respect to the flat metric, $\langle g_{\mu\nu}\rangle_{k_0} = \delta_{\mu\nu}$. The kernel (8.47) satisfies the relation $K(x,x';0) = \delta^d(x-x')$ and, provided that $\lim_{p\to 0} p^2 F(p^2) = 0$, also $\int d^d x\, K(x,x';T) = 1$.

Taking the trace of (8.47) within this 'flat-space approximation' yields [97]

$$P(T) = \int \frac{d^d p}{(2\pi)^d} e^{-p^2 F(p^2)T}. \tag{8.48}$$

Introducing $z = p^2$, the final result for the average return probability reads

$$P(T) = \frac{1}{(4\pi)^{d/2}\Gamma(d/2)} \int_0^\infty dz\, z^{d/2-1} \exp\bigl[-zF(z)T\bigr], \tag{8.49}$$

where $F(z) \equiv \bar{\lambda}(k^2 = z)/\bar{\lambda}_{k_0}$. In the classical case, $F(z) = 1$, the relation (8.49) reproduces the familiar result $P(T) = 1/(4\pi T)^{d/2}$, whence $\mathscr{D}_s(T) = d$ independently of T. We shall now discuss the spectral dimension for several other illustrative and important examples.

8.7.2 The Spectral Dimension in QEG

(A) Let us evaluate the average return probability (8.49) for a simplified RG trajectory where the scale dependence of the cosmological constant is given by a power law, with the same exponent δ for all values of k:

$$\bar{\lambda}_k \propto k^\delta \quad \Longrightarrow \quad F(z) \propto z^{\delta/2}. \tag{8.50}$$

By rescaling the integration variable in (8.49) we see that in this case

$$P(T) = \frac{\text{const}}{T^{d/(2+\delta)}}. \tag{8.51}$$

Hence (8.35) yields the important result

$$\boxed{\mathscr{D}_s(T) = \tfrac{2d}{2+\delta}.} \tag{8.52}$$

It happens to be T-independent, so that for $T \to 0$ trivially $d_s = 2d/(2+\delta)$.

(B) Next, let us be slightly more general and assume that the power law (8.50) is valid only for squared momenta in a certain interval, $p^2 \in [z_1, z_2]$, but $\bar{\lambda}_k$ remains unspecified otherwise. In this case we can obtain only partial information about $P(T)$, namely for T in the interval $[z_2^{-1}, z_1^{-1}]$. The reason is that for $T \in [z_2^{-1}, z_1^{-1}]$ the integral in (8.49) is dominated by momenta for which approximately $1/p^2 \approx T$, i.e., $z \in [z_1, z_2]$. This leads us again to the formula (8.52), which now, however, is valid only for a restricted range of diffusion times T; in particular the spectral dimension of interest may not be given by extrapolating (8.52) to $T \to 0$.

(C) Let us consider an arbitrary asymptotically safe RG trajectory so that its behavior for $k \to \infty$ is controlled by the NGFP. In this case the running of the cosmological constant for $k \gtrsim M$, with M a characteristic mass scale of the order of the Planck mass, is given by a quadratic scale-dependence $\bar{\lambda}_k = \lambda_* k^2$, independently of d. This corresponds to a power law with $\delta = 2$, which entails in the *NGFP regime*, i.e., for $T \lesssim 1/M^2$,

$$\mathscr{D}_s(T) = \frac{d}{2} \quad \text{(NGFP regime)}. \tag{8.53}$$

This dimension, again, is locally T-independent. It coincides with the $T \to 0$ limit:

$$d_s = \frac{d}{2}. \tag{8.54}$$

This is the result first derived in ref. [97]. As it was explained there, it is actually an exact consequence of asymptotic safety which relies solely on the existence of the NGFP and does not depend on the Einstein–Hilbert truncation.

(D) Returning to the Einstein–Hilbert truncation, let us consider the piece of the Type IIIa RG trajectory depicted in Fig. 8.4 which lies inside the linear regime of the GFP. Newton's constant is approximately k-independent there and the cosmological constant evolves according to (8.22). When k is not too small, so that $\bar{\lambda}_0$ can be neglected relative to $\nu \bar{G} k^d$, we are in what we shall call the 'k^d regime'; it is characterized by a pure power law $\bar{\lambda}_k \approx k^\delta$ with $\delta = d$. The physics behind this scale dependence is simple and well-known: It represents the vacuum energy density obtained by summing up the zero-point energies of all field modes integrated out. For T in the range of scales pertaining to the k^d regime we find

$$\mathscr{D}_s(T) = \frac{2d}{2+d} \quad \big(k^d \text{ regime}\big). \tag{8.55}$$

8.7.3 The Walk Dimension in QEG

In order to determine the walk dimension for the diffusion on the effective QEG space-times, we return to Eq. (8.47) for the untraced heat-kernel. We restrict ourselves to a regime with a power-law running of $\bar{\lambda}_k$, whence $F(p^2) = (Lp)^\delta$ with some constant length-scale L.

Introducing $q_\mu \equiv p_\mu T^{1/(2+\delta)}$ and $\xi_\mu \equiv (x_\mu - x'_\mu)/T^{1/(2+\delta)}$, we can rewrite (8.47) in the form

$$K\left(x, x'; T\right) = \frac{1}{T^{d/(2+\delta)}} \Phi\left(\frac{|x - x'|}{T^{1/(2+\delta)}}\right) \tag{8.56}$$

with the function

$$\Phi\left(|\xi|\right) \equiv \int \frac{d^d q}{(2\pi)^d} e^{iq\cdot\xi} e^{-L^\delta q^{2+\delta}}. \tag{8.57}$$

For $\delta = 0$, this obviously reproduces (8.36). From the argument of Φ in (8.56) we infer that $r = |x - x'|$ scales as $T^{1/(2+\delta)}$ so that the walk dimension can be read off as

$$\boxed{\mathscr{D}_w(T) = 2 + \delta.} \tag{8.58}$$

In analogy with the spectral dimension, we use the notation $\mathscr{D}_w(T)$ rather than d_w to indicate that it might refer to an approximate scaling law which is valid for a finite range of scales only.

For $\delta = 0, 2$, and d we find, in particular, for any topological dimension d,

$$\mathscr{D}_w = \begin{cases} 2 & \text{classical regime,} \\ 4 & \text{NGFP regime,} \\ 2 + d & k^d \text{ regime.} \end{cases} \tag{8.59}$$

Regimes with all three walk dimensions of (8.59) can be realized along a single RG trajectory. Again, the result for the NGFP regime, $\mathscr{D}_w = 4$, is exact in the sense that it does not rely on the Einstein–Hilbert truncation.

8.7.4 The Hausdorff Dimension in QEG

The smooth manifold underlying QEG has *per se* no fractal properties whatsoever. In particular, the volume of a d-ball $\mathscr{B}^d$ covering a patch of the smooth manifold of QEG space-time scales as $V(\mathscr{B}^d) = \int_{\mathscr{B}^d} d^d x \sqrt{g_k} \propto (r_k)^d$. Thus, by comparing to Eq. (8.37), we read off that the Hausdorff dimension is strictly equal to the topological one:

$$\boxed{d_H = d.} \tag{8.60}$$

8.7.5 Relations Between Dimensions

(1) The Alexander-Orbach relation. For standard fractals the quantities d_s, d_w, and d_H are not independent but are related by [143]

$$\frac{d_s}{2} = \frac{d_H}{d_w}. \tag{8.61}$$

By combining Eqs. (8.52), (8.58), and (8.60) we see that the same relation holds true for the effective QEG space-times, at least within the Einstein–Hilbert approximation and when the underlying RG trajectory is in a regime with power-law scaling of $\bar{\lambda}_k$. For every value of the exponent δ we have

$$\frac{\mathscr{D}_s(T)}{2} = \frac{d_H}{\mathscr{D}_w(T)}. \tag{8.62}$$

(2) (Non-) Recurrence. The results $d_H = d$, $\mathscr{D}_w = 2 + \delta$ imply that, as soon as $\delta > d - 2$, we have $\mathscr{D}_w > d_H$ and the random walk is *recurrent* then [142]. Classically ($\delta = 0$) this condition is met only in low dimensions $d < 2$, but in the case of the QEG space-times it is always satisfied in the k^d regime ($\delta = d$), for example. So also from this perspective the QEG space-times, due to the specific quantum gravitational dynamics to which they owe their existence, appear to have a dimensionality smaller than their topological one.

(3) Four dimensions are special. It is intriguing that, in the NGFP regime, $\mathscr{D}_w = 4$ independently of d. Hence the walk is recurrent ($\mathscr{D}_w > d_H$) for $d < 4$, non-recurrent for $d > 4$, and the marginal case $\mathscr{D}_w = d_H$ is realized if and only if $d = 4$, making $d = 4$ a distinguished value.

Notably, there is another feature of the QEG space-times which singles out $d = 4$: It is the only dimensionality for which $\mathscr{D}_s(\text{NGFP regime}) = d/2$ coincides with the effective dimension $d_{\text{eff}} = d + \eta_* = 2$ obtained from the scale-dependent graviton propagator (see Sect. 8.5.)

8.8 The RG Running of $\mathscr{D}_s$ and $\mathscr{D}_w$

Let us consider an arbitrary RG trajectory $k \mapsto (g_k, \lambda_k)$, where $g_k \equiv G_k k^{d-2}$ and $\lambda_k \equiv \bar{\lambda}_k k^{-2}$ are the dimensionless Newton constant and cosmological constant, respectively. Along such a RG trajectory there might be isolated intervals of k-values where the cosmological constant evolves according to a power law, $\bar{\lambda}_k \propto k^\delta$, for some constant exponents δ which are not necessarily the same on different such intervals. If the intervals are sufficiently long, it is meaningful to ascribe a spectral and walk dimension to them since $\delta = \text{const}$ implies k-independent values $\mathscr{D}_s = 2d/(2 + \delta)$ and $\mathscr{D}_w = 2 + \delta$.

In between the intervals of approximately constant $\mathscr{D}_s$ and $\mathscr{D}_w$, where the k-dependence of $\bar{\lambda}_k$ is not a power law, the notion of a spectral or walk dimension

might not be meaningful. The concept of a *scale-dependent* dimension $\mathscr{D}_s$ or $\mathscr{D}_w$ is to some extent arbitrary with respect to the way it interpolates between the 'plateaus' on which $\delta = \text{const}$ for some extended period of RG time. While RG methods allow the computation of the $\mathscr{D}_s$ and $\mathscr{D}_w$ values on the various plateaus, it is a matter of convention how to combine them into continuous functions $k \mapsto \mathscr{D}_s(k), \mathscr{D}_w(k)$ which interpolate between the respective values.

(1) The exponent δ as a function on theory space. Next we describe a special proposal for a k-dependent $\mathscr{D}_s(k)$ and $\mathscr{D}_w(k)$ which is motivated by technical simplicity and the general insights it allows. We retain Eqs. (8.52) and (8.58), but promote $\delta \to \delta(k)$ to a k-dependent quantity

$$\delta(k) \equiv k\partial_k \ln(\bar{\lambda}_k). \tag{8.63}$$

When $\bar{\lambda}_k$ satisfies a power law, $\bar{\lambda}_k \propto k^\delta$, this relation reduces to the case of constant δ. If not, δ has its own scale dependence, but no direct physical interpretation should be attributed to it. The particular definition (8.63) has the special property that it actually can be evaluated without first solving for the RG trajectory. The function $\delta(k)$ can be seen as arising from a certain scalar function on theory space, $\delta = \delta(g, \lambda)$, whose k-dependence results from inserting an RG trajectory: $\delta(k) \equiv \delta(g_k, \lambda_k)$. In fact, (8.63) implies $\delta(k) = k\partial_k \ln(k^2\lambda_k) = 2 + \lambda_k^{-1} k\partial_k \lambda_k$ so that $\delta(k) = 2 + \lambda_k^{-1}\beta_\lambda(g_k, \lambda_k)$ upon using the RG-equation $k\partial_k\lambda_k = \beta_\lambda(g, \lambda)$. Thus when we consider δ as a function on theory space, coordinatized by g and λ, it reads

$$\delta(g, \lambda) = 2 + \frac{1}{\lambda}\beta_\lambda(g, \lambda). \tag{8.64}$$

Substituting this relation into (8.52) and (8.58), the spectral and the walk dimensions become functions on the g–λ-plane,

$$\mathscr{D}_s(g, \lambda) = \frac{2d}{4 + \lambda^{-1}\beta_\lambda(g, \lambda)}, \tag{8.65}$$

and

$$\mathscr{D}_w(g, \lambda) = 4 + \lambda^{-1}\beta_\lambda(g, \lambda). \tag{8.66}$$

As we discussed already, the scaling regime of a NGFP has the exponent $\delta = 2$. From Eq. (8.64) we learn that this value is realized at all points (g, λ) where $\beta_\lambda = 0$. The second condition for the NGFP, $\beta_g = 0$, is not required here, so that we have $\delta = 2$ along the entire line in theory space:

$$\mathscr{B} = \big\{(g, \lambda) \mid \beta_\lambda(g, \lambda) = 0\big\}. \tag{8.67}$$

For $d = 4$ the curve $\mathscr{B}$ is shown as the dashed line in Fig. 8.4. Both the GFP $(g, \lambda) = (0, 0)$ and the NGFP, $(g, \lambda) = (g^*, \lambda^*)$, are located on this curve. Furthermore, the turning points T of all Type IIIa trajectories are also situated on $\mathscr{B}$, and the same holds for all the higher-order turning points which occur when the trajectory spirals around the NGFP. The line $\mathscr{B}$ divides the (g, λ)-plane in three domains:

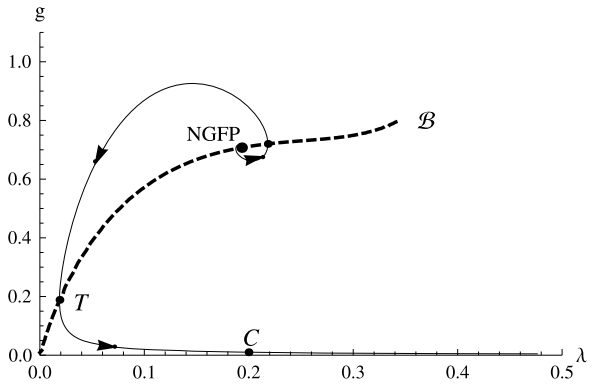

Fig. 8.4 The (g, λ) theory space with the line of turning points, $\mathscr{B}$, and a typical trajectory of Type IIIa. The *arrows* point in the direction of decreasing k. The *big black dot* indicates the NGFP while the *smaller dots* represent points at which the RG trajectory switches from increasing to decreasing λ or vice versa. The point T is the lowest turning point, and C is a typical point within the classical regime. For $\lambda \gtrsim 0.4$, the RG flow leaves the classical regime and is no longer reliably captured by the Einstein–Hilbert truncation

(i) Above $\mathscr{B}$: $\beta_\lambda > 0$, $\delta > 2 \Rightarrow \mathscr{D}_s < d/2$, $\mathscr{D}_w > 4$. (ii) Below $\mathscr{B}$: $\beta_\lambda < 0$, $\delta < 2 \Rightarrow \mathscr{D}_s > d/2$, $\mathscr{D}_w < 4$. (iii) On $\mathscr{B}$: $\beta_\lambda = 0$, $\delta = 2 \Rightarrow \mathscr{D}_s = d/2$, $\mathscr{D}_w = 4$. This observation leads us to an important conclusion: The values $\delta = 2 \Longleftrightarrow \mathscr{D}_s = d/2$, $\mathscr{D}_w = 4$ which (without involving any truncation) are found in the NGFP regime, actually also apply to all points $(g, \lambda) \in \mathscr{B}$, provided the Einstein–Hilbert truncation is reliable and no matter is included.

(2) Running dimensions along a RG trajectory. We proceed by investigating how the spectral and walk dimension of the effective QEG space-times changes along a given RG trajectory. As discussed above, our interest is in scaling regimes where $\mathscr{D}_s$ and $\mathscr{D}_w$ remain (approximately) constant for a long interval of k-values. For the remainder of this section, we will restrict ourselves to the Einstein–Hilbert truncation in $d = 4$.

We start by numerically solving the coupled differential equations (8.18) with the β-functions from [11] for a series of initial conditions keeping $\lambda_{\text{init}} = \lambda(k_0) = 0.2$ fixed and successively lowering $g_{\text{init}} = g(k_0)$. The result is a family of RG trajectories where the classical regime becomes more and more pronounced. Subsequently, these solutions are substituted into (8.65) and (8.66), which give $\mathscr{D}_s(t; g_{\text{init}}, \lambda_{\text{init}})$ and $\mathscr{D}_w(t; g_{\text{init}}, \lambda_{\text{init}})$ in dependence of the RG-time $t \equiv \ln(k)$ and the RG trajectory. One can verify explicitly that substituting the RG trajectory into the return probability (8.49) and computing the spectral dimension from (8.34) by carrying out the resulting integrals numerically gives rise to the same picture.

Figure 8.5 shows the resulting spectral dimension and the localization of the plateau-regimes on the RG trajectory. In the left diagram, g_{init} decreases by one order of magnitude for each shown trajectory, starting with the highest value to the very left. As a central result, Fig. 8.5 establishes that the RG flow gives rise to *three* plateaus where $\mathscr{D}_s(t)$ and $\mathscr{D}_w(t)$ are approximately constant:

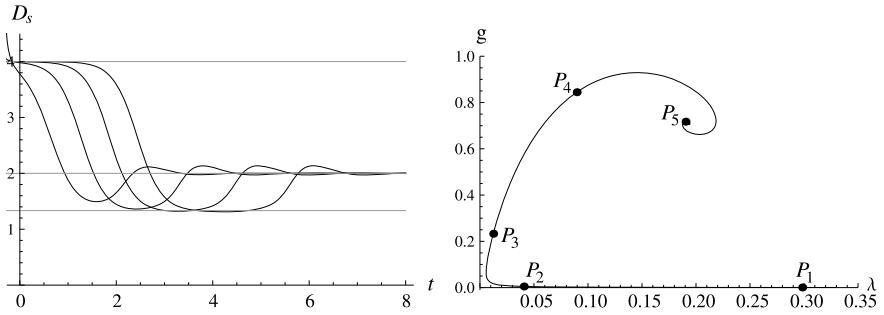

Fig. 8.5 The $t \equiv \ln(k)$-dependent spectral dimension along illustrative solutions of the RG-equations (8.18) in $d = 4$. The trajectories develop three plateaus: the classical plateau with $\mathscr{D}_s = 4, \mathscr{D}_w = 2$, the semi-classical plateau where $\mathscr{D}_s = 4/3, \mathscr{D}_w = 6$ and the NGFP plateau with $\mathscr{D}_s = 2, \mathscr{D}_w = 4$. (Recall that $\mathscr{D}_w = 2d/\mathscr{D}_s = 8/\mathscr{D}_s$.) The plateau values are indicated by the horizontal lines. The second figure shows the location of these plateaus on the RG trajectory: the classical, k^4, and NGFP regime appear between the points P_1 and P_2, P_3 and P_4, and above P_5, respectively

(i) For small values k, below $t \simeq 1.8$, say, one finds a *classical plateau* where $\mathscr{D}_s = 4, \mathscr{D}_w = 2$ for a long range of k-values. Here $\delta = 0$, indicating that the cosmological constant is indeed constant.
(ii) Following the RG flow towards the UV (larger values of t) one next encounters the *semi-classical plateau* where $\mathscr{D}_s = 4/3, \mathscr{D}_w = 6$. In this case $\delta(k) = 4$ so that $\bar{\lambda}_k \propto k^4$ on the corresponding part of the RG trajectory.
(iii) Finally, the *NGFP plateau* is characterized by $\mathscr{D}_s = 2, \mathscr{D}_w = 4$, which results from the scale-dependence of the cosmological constant at the NGFP $\bar{\lambda}_k \propto k^2 \Longleftrightarrow \delta = 2$.

The plateaus become more and more extended the closer the trajectory's turning point T gets to the GFP, i.e., the smaller the IR value of the cosmological constant.

8.9 Matching the Spectral Dimensions of QEG and CDT

The key advantage of the spectral dimension $\mathscr{D}_s(T)$ is that it may be defined and computed within various *a priori* unrelated approaches to quantum gravity. In particular, it is easily accessible in Monte Carlo simulations of the causal dynamical triangulations (CDT) approach in $d = 4$ [90–92] and $d = 3$ [94] as well as in Euclidean dynamical triangulations (EDT) [98]. This feature allows a direct comparison between $\mathscr{D}_s^{\rm CDT}(T)$ and $\mathscr{D}_s^{\rm EDT}(T)$ obtained within the discrete approaches and $\mathscr{D}_s^{\rm QEG}(T)$ capturing the fractal properties of the QEG effective space-times. In [99] we carried out this analysis for $d = 3$, using the Monte Carlo data obtained in [94] according to the following scheme:

(i) First, we numerically construct a RG trajectory $g_k(g_0, \lambda_0), \lambda_k(g_0, \lambda_0)$ depending on the initial conditions g_0, λ_0, by solving the flow equations (8.18).

Table 8.1 Initial conditions $g_0^{\rm fit}, \lambda_0^{\rm fit}$ for the RG trajectory providing the best fit to the Monte Carlo data [94]. The fit-quality $(\Delta\mathscr{D}_s)^2$, given by the sum of the squared residues, improves systematically when increasing the number of simplices in the triangulation

	$g_0^{\rm fit}$	$\lambda_0^{\rm fit}$	$(\Delta\mathscr{D}_s)^2$
70k	0.7×10^{-5}	7.5×10^{-5}	0.680
100k	8.8×10^{-5}	39.5×10^{-5}	0.318
200k	13×10^{-5}	61×10^{-5}	0.257

(ii) We evaluate the resulting spectral dimension $\mathscr{D}_s^{\rm QEG}(T; g_0, \lambda_0)$ of the corresponding effective QEG space-time. This is done by first finding the return probability $P(T; g_0, \lambda_0)$, Eq. (8.49), for the RG trajectory under consideration and then substituting the resulting expression into (8.35). The spectral dimension constructed in this way depends not only on the length of the random walk but also on the initial conditions of the RG trajectory.

(iii) We determine the RG trajectory underlying the CDT-simulations by fitting the parameters g_0, λ_0 to the Monte Carlo data. The corresponding best-fit values are obtained via an ordinary least-squares fit, minimizing the squared Euclidean distance

$$(\Delta\mathscr{D}_s)^2 \equiv \sum_{T=20}^{500} \left[\mathscr{D}_s^{\rm QEG}\left(T; g_0^{\rm fit}, \lambda_0^{\rm fit}\right) - \mathscr{D}_s^{\rm CDT}(T)\right]^2, \tag{8.68}$$

between the (continuous) function $\mathscr{D}_s^{\rm QEG}(T; g_0, \lambda_0)$ and the points $\mathscr{D}_s^{\rm CDT}(T)$. We thereby restrict ourselves to the random walks with discrete, integer length $20 \leq T \leq 500$, which constitute the 'reliable' part of the data.

The resulting best-fit values $g_0^{\rm fit}, \lambda_0^{\rm fit}$ for triangulations with $N = 70{,}000$, $N = 100{,}000$, and $N = 200{,}000$ simplices are collected in Table 8.1. Notably, the sum over the squared residuals in the third column of the table improves systematically with an increasing number of simplices. By integrating the flow equation for $g(k), \lambda(k)$ for the best-fit initial conditions one furthermore observes that the points $g_0^{\rm fit}, \lambda_0^{\rm fit}$ are actually located on *different* RG trajectories. Increasing the size of the simulation N leads to a mild but systematic increase of the distance between the turning point T and the GFP of the corresponding best-fit trajectories.

Figure 8.6 then shows the direct comparison between the spectral dimensions obtained by the simulations (continuous curves) and the best-fit QEG trajectories (dashed curves) for 70k, 100k and 200k in the upper left, upper right and lower left panel, respectively. This data is complemented by the relative error

$$\varepsilon \equiv -\frac{\mathscr{D}_s^{\rm QEG}(T; g_0^{\rm fit}, \lambda_0^{\rm fit}) - \mathscr{D}_s^{\rm CDT}(T)}{\mathscr{D}_s^{\rm QEG}(T; g_0^{\rm fit}, \lambda_0^{\rm fit})} \tag{8.69}$$

for the three fits in the lower right panel. The 70k data still shows a systematic deviation from the classical value $\mathscr{D}_s(T) = 3$ for long random walks, which is not present

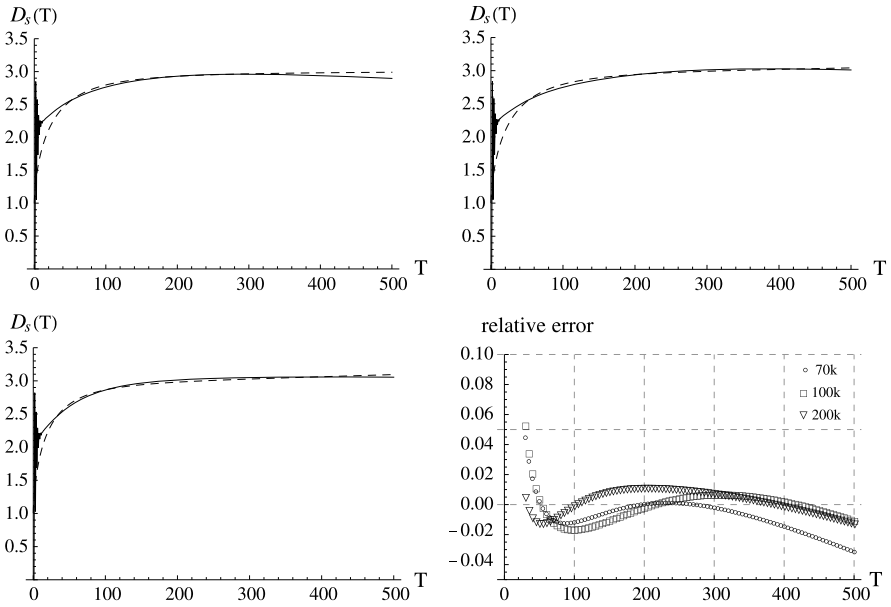

Fig. 8.6 Comparison between the spectral dimension measured in 3-dimensional CDT space–times build from 70k (*upper left*), 100k (*upper right*), and 200k simplices (*lower left*) obtained in [94] (*continuous curves*) and the best fit values for $\mathscr{D}_s^{\rm QEG}(T; g_0^{\rm fit}, \lambda_0^{\rm fit})$ (*dashed curves*). The relative errors for the fits to the CDT-datasets with $N = 70{,}000$ (*circles*), $N = 100{,}000$ (*squares*) and $N = 200{,}000$ (*triangles*) simplices are shown in the *lower right*. The residuals growth for very small and very large durations T of the random walk, consistent with discreteness effects at small distances and the compactness of the simulation for large values of T, respectively. The quality of the fit improves systematically for triangulations containing more simplices. For the $N = 200$k data the relative error is ≈ 1 %

in the QEG results. This mismatch decreases systematically for larger triangulations where the classical regime becomes more and more pronounced. Nevertheless and most remarkably we find that for the 200k-triangulation $\varepsilon \lesssim 1$ %, throughout.

We conclude this section by extending $\mathscr{D}_s^{\rm QEG}(T; g_0^{\rm fit}, \lambda_0^{\rm fit})$ obtained from the 200k data to the region of very short random walks $T < 20$. The result is depicted in Fig. 8.7 which displays $\mathscr{D}_s^{\rm CDT}(T)$ (continuous curve) and $\mathscr{D}_s^{\rm QEG}(T; g_0^{\rm fit}, \lambda_0^{\rm fit})$ (dashed curve) as a function of $\log(T)$. Similarly to the four-dimensional case discussed in Fig. 8.5, the function $\mathscr{D}_s^{\rm QEG}(T; g_0^{\rm fit}, \lambda_0^{\rm fit})$ obtained for $d = 3$ develops three plateaus where the spectral dimension is approximately constant over a long T-interval. For successively decreasing duration of the random walks, these plateaus correspond to the classical regime $\mathscr{D}_s^{\rm QEG}(T) = 3$, the semi-classical regime where $\mathscr{D}_s^{\rm QEG}(T) \approx 1$ and the NGFP regime where $\mathscr{D}_s^{\rm QEG}(T) = 3/2$. The figure illustrates that $\mathscr{D}_s^{\rm CDT}(T)$ probes the classical regime and part of the first crossover towards the semi-classical regime only. This is in perfect agreement with the assertion [94] that the present simulations do not yet probe structures below the Planck scale. This assessment resolves the apparent contradiction between the extrapolation re-

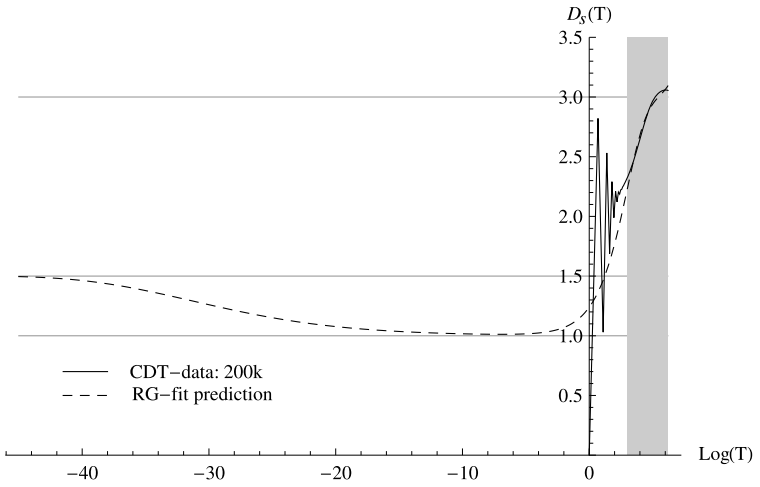

Fig. 8.7 Comparison between the spectral dimensions obtained from the dynamical triangulation with 200k simplices (*continuous curve*) and the corresponding $\mathscr{D}_s^{\rm QEG}(T; g_0^{\rm fit}, \lambda_0^{\rm fit})$ predicted by QEG (*dashed curve*). In the latter case, the scaling regime corresponding to the NGFP is reached for $\log(T) < -40$, which is well below the distance scales probed by the Monte Carlo simulation

sult $\lim_{T\to 0} \mathscr{D}_s^{\rm CDT}(T) \approx 2$ and the QEG prediction $\lim_{T\to 0} \mathscr{D}_s^{\rm QEG}(T) = 3/2$. Performing the extrapolation of $\lim_{T\to 0} \mathscr{D}_s^{\rm CDT}(T)$ based on the leading corrections to the classical regime does not reliably identify the signature of a non-Gaussian fixed point in $\mathscr{D}_s(T)$.

A similar conclusion also holds true in four dimensions. Comparing the profiles of $\mathscr{D}_s^{\rm QEG}(T)$ shown in Fig. 8.5 with the fitting functions used in the CDT [90–92] or EDT [98] simulations shows that all the Monte Carlo data points obtained are positioned on the *infrared* side of the turning point of the RG trajectories underlying the QEG effective space-times. They neither probe the semi-classical plateau nor the scaling regime of the NGFP. Depending on where the data are cut off, one obtains different tangents to the first crossover, which lead to widely different extrapolations for the value $d_s = \mathscr{D}_s(T)|_{T=0}$. We believe that this is actually at the heart of the apparent mismatch in the spectral dimension for infinitesimal random walks reported from the CDT and EDT computations.

8.10 Asymptotic Safety in Cosmology

At this point we switch to another field where QEG effects might be relevant, the cosmology of the early Universe. As we discussed at the end of Sect. 8.4, the Type IIIa trajectories displayed in Fig. 8.2 possess all the qualitative properties one would expect from the RG trajectory describing gravitational phenomena in the real Universe. They can have a long classical regime and a small, positive cosmological constant in the infrared. Remarkably, along the RG trajectory realized by Nature [79–

81, 133], the dimensionful running cosmological constant $\bar{\lambda}(k)$ changes by about 120 orders of magnitude between k-values of the order of the Planck mass and macroscopic scales, while the dimensionful Newton constant $G(k)$ has no strong k-dependence in this regime. For $k > m_{\rm Pl}$, the scale dependence of $G(k)$ and $\bar{\lambda}(k)$ is governed by the NGFP, implying that $\bar{\lambda}(k)$ diverges and $G(k)$ approaches zero, see Eq. (8.21). An immediate question is whether there is any experimental or observational evidence that would hint at this enormous scale dependence of the gravitational parameters. Clearly, the natural place to search for such phenomena is cosmology.

8.10.1 RG Improved Einstein Equations

The computational setting for investigating the signatures arising from the scale-dependent couplings are the RG improved Einstein equations: By means of a suitable cutoff identification $k = k(t)$ we turn the scale dependence of $G(k)$ and $\bar{\lambda}(k)$ into a time dependence, and then substitute the resulting $G(t) \equiv G[k(t)]$ and $\bar{\lambda}(t) \equiv \bar{\lambda}[k(t)]$ into the Einstein equations $G_{\mu\nu} = -\bar{\lambda}(t) g_{\mu\nu} + 8\pi G(t) T_{\mu\nu}$. We specialize $g_{\mu\nu}$ to describe a spatially flat ($K = 0$) Robertson–Walker (FRW) metric with scale factor $a(t)$, and we take $T_\mu{}^\nu = \mathrm{diag}[-\rho, p, p, p]$ to be the energy-momentum tensor of an ideal fluid with equation of state $p = w\rho$, where $w > -1$ is constant. Then the improved Einstein equation boils down to the modified Friedmann equation and a continuity equation:

$$H^2 = \frac{8\pi}{3} G(t)\rho + \frac{1}{3}\bar{\lambda}(t), \tag{8.70a}$$

$$\dot{\rho} + 3H(\rho + p) = -\frac{\dot{\bar{\lambda}} + 8\pi\rho\dot{G}}{8\pi G}. \tag{8.70b}$$

The modified continuity equation (8.70b) is the integrability condition for the improved Einstein equation implied by Bianchi identity, $D^\mu[\bar{\lambda}(t) g_{\mu\nu} - 8\pi G(t) T_{\mu\nu}] = 0$. It describes the energy exchange between the matter and gravitational degrees of freedom (geometry). For later use let us note that upon defining the critical density $\rho_{\rm crit}(t) \equiv 3H(t)^2/[8\pi G(t)]$, the relative density $\Omega_{\rm M} \equiv \rho/\rho_{\rm crit}$ and $\Omega_{\bar{\lambda}} = \rho_{\bar{\lambda}}/\rho_{\rm crit}$ the modified Friedmann equation (8.70a) can be written as $\Omega_{\rm M}(t) + \Omega_{\bar{\lambda}}(t) = 1$.

8.10.2 Solving the RG Improved Einstein Equations

The general strategy for solving Eqs. (8.70a), (8.70b) is as follows. First we obtain $G(k)$ and $\bar{\lambda}(k)$ by solving the flow equation in the Einstein–Hilbert truncation before constructing the cosmologies by numerically solving the RG improved evolution equations. We shall employ the cutoff identification $k(t) = \xi H(t)$, where ξ is a

fixed positive constant of order unity. This is a natural choice since in a Robertson–Walker geometry the Hubble parameter measures the curvature of space-time; its inverse H^{-1} defines the size of the 'Einstein elevator'.

The very early part of the cosmology can be described analytically. For $k \to \infty$ the trajectory approaches the NGFP so that $G(k) = g^*/k^2$ and $\bar{\lambda}(k) = \lambda^* k^2$. In this case the differential equation can be solved analytically, with the result

$$H(t) = \frac{\alpha}{t}, \qquad a(t) = At^{\alpha}, \qquad \alpha = \left[\frac{1}{2}(3+3w)\left(1-\Omega_{\bar{\lambda}}^*\right)\right]^{-1}, \tag{8.71}$$

and $\rho(t) = \widehat{\rho} t^{-4}$, $G(t) = \widehat{G} t^2$, $\bar{\lambda}(t) = \widehat{\bar{\lambda}}/t^2$. Here A, $\widehat{\rho}$, $\widehat{G}$, and $\widehat{\bar{\lambda}}$ are positive constants. They parametrically depend on the relative vacuum energy density in the fixed point regime, $\Omega_{\bar{\lambda}}^*$, which assumes values in the interval $(0, 1)$. If $\alpha > 1$ the deceleration parameter $q = \alpha^{-1} - 1$ is negative and the Universe is in a phase of *power-law inflation*. Furthermore, it has *no particle horizon* if $\alpha \geq 1$, but does have a horizon of radius $d_H = t/(1-\alpha)$ if $\alpha < 1$. In the case of $w = 1/3$ this means that there is a horizon for $\Omega_{\bar{\lambda}}^* < 1/2$, but none if $\Omega_{\bar{\lambda}}^* \geq 1/2$.

8.10.3 Inflation in the Fixed-Point Regime

Next we discuss in more detail the cosmologies originating from the epoch of power-law inflation which is realized in the NGFP regime if $\Omega_{\bar{\lambda}}^* > 1/2$. Since the transition from the fixed point to the classical FRW regime is rather sharp, it will be sufficient to approximate the RG improved UV cosmologies by the following caricature: For $0 < t < t_{\rm tr}$, the scale factor behaves as $a(t) \propto t^{\alpha}$, $\alpha > 1$. Here $\alpha = (2 - 2\Omega_{\bar{\lambda}}^*)^{-1}$ since $w = 1/3$ will be assumed. Thereafter, for $t > t_{\rm tr}$, we have a classical, entirely matter-driven expansion $a(t) \propto t^{1/2}$. Clearly this is a very attractive scenario: *neither to trigger inflation nor to stop it one needs any ad hoc ingredients such as an inflaton field or a special potential*. It suffices to include the leading quantum effects in the gravity + matter system. Following [79–81], the RG improved cosmological evolution for the RG trajectory realized by Nature is characterized as follows:

(A) The transition time $t_{\rm tr}$ is dictated by the RG trajectory. It leaves the asymptotic scaling regime near $k \approx m_{\rm Pl}$. Hence $H(t_{\rm tr}) \approx m_{\rm Pl}$ and since $\xi = O(1)$ and $H(t) = \alpha/t$, we find the estimate

$$t_{\rm tr} = \alpha t_{\rm Pl}. \tag{8.72}$$

Here, as always, the Planck mass, time, and length are defined in terms of the value of Newton's constant in the classical regime: $t_{\rm Pl} = \ell_{\rm Pl} = m_{\rm Pl}^{-1} = \bar{G}^{1/2} = G_{\rm observed}^{1/2}$. Let us now assume that $\Omega_{\bar{\lambda}}^*$ is very close to 1 so that α is large: $\alpha \gg 1$. Then (8.72) implies that the transition takes place at a cosmological time which is much later than the Planck time. At the transition the *Hubble parameter* is of order $m_{\rm Pl}$, but

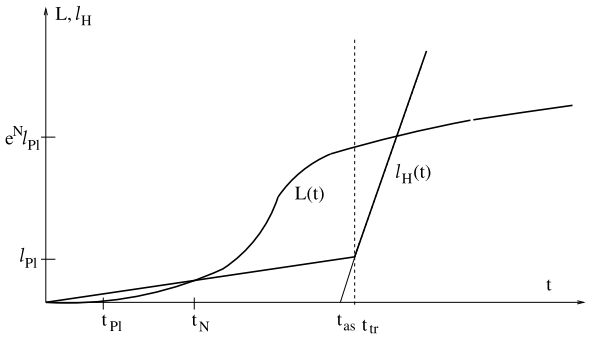

Fig. 8.8 The proper length L and the Hubble radius as a function of time. The NGFP and FRW cosmologies are valid for $t < t_{\rm tr}$ and $t > t_{\rm tr}$, respectively. The classical cosmology has an apparent initial singularity at $t_{\rm as}$ outside its domain of validity. Structures of size $e^N \ell_{\rm Pl}$ at $t_{\rm tr}$ cross the Hubble radius at t_N, a time which can be larger than the Planck time

the *cosmological time* is in general not of the order of $t_{\rm Pl}$. Stated differently, the 'Planck time' is *not* the time at which H and the related physical quantities assume Planckian values. The Planck time as defined above is well within the NGFP regime: $t_{\rm Pl} = t_{\rm tr}/\alpha \ll t_{\rm tr}$.

In the NGFP regime $0 < t < t_{\rm tr}$ the Hubble radius $\ell_H(t) \equiv 1/H(t)$, i.e., $\ell_H(t) = t/\alpha$, increases linearly with time but, for $\alpha \gg 1$, with a very small slope. At the transition, $t = t_{\rm tr}$, the NGFP solution is to be matched continuously with a FRW cosmology (with vanishing cosmological constant). We may use the classical formula $a \propto \sqrt{t}$ for the scale factor, but we must shift the time axis on the classical side such that a, H, and then as a result of (8.70a), also ρ are continuous at $t_{\rm tr}$. Therefore, $a(t) \propto (t - t_{\rm as})^{1/2}$ and $H(t) = \frac{1}{2}(t - t_{\rm as})^{-1}$ for $t > t_{\rm tr}$. Equating this Hubble parameter at $t = t_{\rm tr}$ to $H(t) = \alpha/t$, valid in the NGFP regime, we find that the shift $t_{\rm as}$ must be chosen as $t_{\rm as} = (\alpha - \frac{1}{2})t_{\rm Pl} = (1 - \frac{1}{2\alpha})t_{\rm tr} < t_{\rm tr}$. Here the subscript 'as' stands for 'apparent singularity'. This is to indicate that if one continues the classical cosmology to times $t < t_{\rm tr}$, it has an initial singularity ('big bang') at $t = t_{\rm as}$. Since, however, the FRW solution is not valid there, nothing special happens at $t_{\rm as}$; the true initial singularity is located at $t = 0$ in the NGFP regime; see Fig. 8.8.

(B) We now consider some structure of comoving length Δx, a single wavelength of a density perturbation, for instance. The corresponding physical, i.e., proper length is $L(t) = a(t)\Delta x$ then. In the NGFP regime it has the time dependence $L(t) = (t/t_{\rm tr})^{\alpha} L(t_{\rm tr})$. The ratio of $L(t)$ and the Hubble radius evolves according to $L(t)/\ell_{\rm H}(t) = (t/t_{\rm tr})^{\alpha-1} L(t_{\rm tr})/\ell_{\rm H}(t_{\rm tr})$. For $\alpha > 1$, i.e., $\Omega^*_{\bar{\lambda}} > 1/2$, the proper length of any object grows faster than the Hubble radius. So objects which are of 'sub-Hubble' size at early times can cross the Hubble radius and become 'super-Hubble' at later times; see Fig. 8.8.

Let us focus on a structure which, at $t = t_{\rm tr}$, is e^N times larger than the Hubble radius. Before the transition we have $L(t)/\ell_{\rm H}(t) = e^N (t/t_{\rm tr})^{\alpha-1}$. Assuming $e^N > 1$, there exists a time $t_N < t_{\rm tr}$ at which $L(t_N) = \ell_{\rm H}(t_N)$, so that the structure considered

'crosses' the Hubble radius at the time t_N. It is given by

$$t_N = t_{\rm tr} \exp\left(-\frac{N}{\alpha - 1}\right). \tag{8.73}$$

What is remarkable about this result is that, even with rather moderate values of α, one can easily 'inflate' structures to a size which is by many e-folds larger than the Hubble radius *during a very short time interval at the end of the NGFP epoch*.

The largest structures in the present Universe, evolved backward in time by the classical equations to the point where $H = m_{\rm Pl}$, have a size of about $e^{60}\ell_{\rm Pl}$ there. We can use (8.73) with $N = 60$ to find the time t_{60} at which those structures crossed the Hubble radius. With $\alpha = 25$ the result is $t_{60} = 2.05 t_{\rm Pl} = t_{\rm tr}/12.2$. Remarkably, t_{60} is smaller than $t_{\rm tr}$ by one order of magnitude only. As a consequence, the physical conditions prevailing at the time of the crossing are not overly 'exotic' yet. The Hubble parameter, for instance, is only one order of magnitude larger than at the transition: $H(t_{60}) \approx 12 m_{\rm Pl}$. The same is true for the temperature; one can show that $T(t_{60}) \approx 12 T(t_{\rm tr})$ where $T(t_{\rm tr})$ is of the order of $m_{\rm Pl}$. Note that t_{60} is larger than $t_{\rm Pl}$.

(C) QEG offers a natural mechanism for generating primordial fluctuations during the NGFP epoch. The idea is that the NGFP amounts to a kind of 'critical phenomenon' with characteristic fluctuations on all scales. They turn out to have a scale-free spectrum with a spectral index close to $n = 1$. For a detailed discussion of this mechanism the reader is referred to [15, 77–81]. Suffice it to say that the quantum mechanical generation of the primordial fluctuations makes essential use of the dimensionally reduced form of the graviton propagator; it happens on sub-Hubble distance scales. However, thanks to the inflationary NGFP era the modes relevant to cosmological structure formation were indeed smaller than the Hubble radius at a sufficiently early time, for $t < t_{60}$, say. (See the $L(t)$ curve in Fig. 8.8.)

8.10.4 Entropy and the Renormalization Group

In standard Friedmann–Robertson–Walker cosmology where the expansion is adiabatic, the entropy (within a comoving volume) is constant. It has always been somewhat puzzling therefore where the huge amount of entropy contained in the present Universe comes from. Presumably it is dominated by the cosmic microwave background radiation (CMBR) photons which contribute an amount of about 10^{88} to the entropy within the present Hubble sphere.

The observation that the value of the cosmological constant decreases during the expansion of the universe hints at another mechanism at work within the RG improved cosmologies: the dynamical creation of entropy. Following [79–81] we shall argue that in principle the entire entropy of the massless fields in the present Universe can be understood as arising from this effect. If energy can be exchanged freely between the cosmological constant and the matter degrees of freedom, the

entropy observed today is obtained precisely if the initial entropy at the big bang vanishes. The assumption that the matter system must allow for an unhindered energy exchange with $\bar{\lambda}$ is essential; see refs. [77–81].

To make the argument as transparent as possible, let us first consider a Universe without matter, but with a positive $\bar{\lambda}$. Assuming maximal symmetry, this is nothing but de Sitter space, of course. In static coordinates its metric is given by $ds^2 = -[1 + 2\Phi_{\rm N}(r)]dt^2 + [1 + 2\Phi_{\rm N}(r)]^{-1}dr^2 + r^2(d\theta^2 + \sin^2\theta d\phi^2)$ with $\Phi_{\rm N}(r) = -\frac{1}{6}\bar{\lambda}r^2$. In the weak field and slow motion limit $\Phi_{\rm N}(r)$ has the interpretation of a Newtonian potential; for $\bar{\lambda} > 0$ it is an upside-down parabola. Point particles in this space-time 'roll down the hill' and are rapidly driven away from the origin $r = 0$ and from any other particle. Now assume that the magnitude of $|\bar{\lambda}|$ is slowly ('adiabatically') decreased. This will cause the potential $\Phi_{\rm N}(r)$ to move upward as a whole, its slope decreases. So the change in $\bar{\lambda}$ increases the particle's potential energy. This is the simplest way of understanding that a *positive decreasing* cosmological constant has the effect of 'pumping' energy into the matter degrees of freedom.

We are thus led to suspect that, because of the decreasing cosmological constant, there is a continuous inflow of energy into the cosmological fluid contained in an expanding Universe. It will 'heat up' the fluid or, more exactly, lead to a slower decrease of the temperature than in standard cosmology. Furthermore, by elementary thermodynamics, it will *increase* the entropy of the fluid. If during the time dt an amount of heat $dQ > 0$ is transferred into a volume V at the temperature T the entropy changes by an amount $dS = dQ/T > 0$. To be as conservative (i.e., close to standard cosmology) as possible, we assume that this process is reversible. If not, dS is even larger.

In order to quantify this argument, we model the matter in the early Universe by a gas with $n_{\rm b}$ bosonic and $n_{\rm f}$ fermionic massless degrees of freedom, all at the same temperature. *In equilibrium* its energy density, pressure, and entropy density are given by the usual relations (here $n_{\rm eff} = n_{\rm b} + \frac{7}{8}n_{\rm f}$)

$$\rho = 3p = \frac{\pi^2}{30} n_{\rm eff} T^4, \tag{8.74a}$$

$$s = \frac{2\pi^2}{45} n_{\rm eff} T^3, \tag{8.74b}$$

so that in terms of $U \equiv \rho V$ and $S \equiv sV$,

$$T\,dS = dU + p\,dV. \tag{8.74c}$$

In an out-of-equilibrium process of entropy generation the question arises how the various thermodynamical quantities are related then. To be as conservative as possible, we make the assumption that the irreversible inflow of energy destroys thermal equilibrium as little as possible in the sense that the equilibrium relations (8.74a)–(8.74c) continue to be (approximately) valid. Such minimally non-adiabatic processes were termed 'adiabatic' (with the quotation marks) in ref. [144, 145].

8.10.5 Primordial Entropy Generation

Let us return to the modified continuity equation (8.70b). After multiplication by a^3 it reads

$$\left[\dot{\rho} + 3H(\rho + p)\right]a^3 = \widetilde{\mathscr{P}}(t), \tag{8.75}$$

where we defined

$$\widetilde{\mathscr{P}} \equiv -\left(\frac{\dot{\bar{\lambda}} + 8\pi\rho\dot{G}}{8\pi G}\right)a^3. \tag{8.76}$$

Without assuming any particular equation of state, Eq. (8.75) can be rewritten as

$$\frac{d}{dt}\left(\rho a^3\right) + p\frac{d}{dt}\left(a^3\right) = \widetilde{\mathscr{P}}(t). \tag{8.77}$$

The interpretation of this equation is as follows. Let us consider a unit *coordinate*, i.e., comoving volume in the Robertson–Walker space-time. Its corresponding *proper* volume is $V = a^3$ and its energy contents is $U = \rho a^3$. The rate of change of these quantities is subject to (8.77):

$$\frac{dU}{dt} + p\frac{dV}{dt} = \widetilde{\mathscr{P}}(t). \tag{8.78}$$

In classical cosmology where $\widetilde{\mathscr{P}} \equiv 0$ this equation together with the standard thermodynamic relation $dU + pdV = TdS$ is used to conclude that the expansion of the Universe is adiabatic, i.e., the entropy inside a comoving volume does not change as the Universe expands, $dS/dt = 0$.

When $\bar{\lambda}$ and G are time dependent, $\widetilde{\mathscr{P}}$ is non-zero and we interpret (8.78) as describing the process of energy (or 'heat') exchange between the scalar fields $\bar{\lambda}$ and G and the ordinary matter. This interaction causes S to change,

$$T\frac{dS}{dt} = T\frac{d}{dt}\left(sa^3\right) = \widetilde{\mathscr{P}}(t), \tag{8.79}$$

where here and in the following we write $S \equiv sa^3$ for the entropy carried by the matter inside a unit comoving volume and s for the corresponding proper entropy density. The actual rate of change of the comoving entropy is

$$\frac{dS}{dt} = \frac{d}{dt}\left(sa^3\right) = \mathscr{P}(t), \tag{8.80}$$

where $\mathscr{P} \equiv \widetilde{\mathscr{P}}/T$. If T is known as a function of t we can integrate (8.79) to obtain $S = S(t)$. In the RG improved cosmologies the entropy production rate per comoving volume

$$\mathscr{P}(t) = -\left[\frac{\dot{\bar{\lambda}} + 8\pi\rho\dot{G}}{8\pi G}\right]\frac{a^3}{T} \tag{8.81}$$

is non-zero because the gravitational 'constants' $\bar{\lambda}$ and G have acquired a time dependence.

Clearly we can convert the heat exchanged, TdS, to an entropy change only if the dependence of the temperature T on the other thermodynamical quantities, in particular ρ and p is known. For this reason we shall now make the following assumption about the matter system and its (non-equilibrium!) dynamics:

The matter system is assumed to consist of $n_{\rm eff}$ species of effectively massless degrees of freedom which all have the same temperature T. The equation of state is $p = \rho/3$, i.e., $w = 1/3$, and ρ depends on T as

$$\rho(T) = \kappa^4 T^4, \qquad \kappa \equiv \left(\frac{\pi^2}{30} n_{\rm eff}\right)^{1/4}. \tag{8.82}$$

No assumption is made about the relation $s = s(T)$.

The first assumption, radiation dominance and equal temperature, is plausible since we shall find that there is no significant entropy production any more once $H(t)$ has dropped substantially below $m_{\rm Pl}$. The second assumption, Eq. (8.82), amounts to the hypothesis formulated above, the approximate validity of the *equilibrium* relations among ρ, p, and T.

Note that while we used (8.74c) in relating $\mathscr{P}(t)$ to the entropy production and also postulated Eq. (8.74a), we do not assume the validity of the formula for the entropy density, Eq. (8.74b), *a priori*. We shall see that the latter is an automatic consequence of the cosmological equations. To make the picture as clear as possible we shall neglect in the following all ordinary dissipative processes in the cosmological fluid.

Using $p = \rho/3$ and (8.82) the entropy production rate can be seen to be a total time derivative, $\mathscr{P}(t) = d/dt[(4/3)\kappa a^3 \rho^{3/4}]$. Therefore we can immediately integrate (8.79) and obtain

$$S(t) = \frac{4}{3}\kappa a^3 \rho^{3/4} + S_{\rm c}, \tag{8.83}$$

or, in terms of the proper entropy density, $s(t) = (4/3)\kappa\rho(t)^{3/4} + S_{\rm c}/a(t)^3$. Here $S_{\rm c}$ is a constant of integration. In terms of T, using (8.82) again,

$$s(t) = \frac{2\pi^2}{45} n_{\rm eff} T(t)^3 + \frac{S_{\rm c}}{a(t)^3}. \tag{8.84}$$

The final result (8.84) is very remarkable for at least two reasons. First, for $S_{\rm c} = 0$, Eq. (8.84) has exactly the form (8.74b) which is valid for radiation in equilibrium. Note that we did not postulate this relationship, only the $\rho(T)$-law was assumed. The equilibrium formula $s \propto T^3$ was *derived* from the cosmological equations, i.e., the modified conservation law. This result makes the hypothesis 'non-adiabatic, but as little as possible' self-consistent. Second, if $\lim_{t\to 0} a(t)\rho(t)^{1/4} = 0$, which is actually the case for the most interesting class of cosmologies we shall find, then $S(t \to 0) = S_c$ by Eq. (8.83). As we mentioned in the introduction, the most plausible initial value of S is $S = 0$ which means a vanishing constant of integration

S_c here. But then, with $S_c = 0$, Eq. (8.83) tells us that *the entire entropy carried by the massless degrees of freedom today (CMBR photons) is due to the RG running*.

8.10.6 Entropy Production for RG Trajectory Realized by Nature

Substituting the NGFP solution (8.71) for $w = 1/3$ the entropy production rate (8.81) reads $\mathscr{P}(t) = 4\kappa(\alpha - 1)A^3\widehat{\rho}^{3/4}t^{3\alpha-4}$. For the entropy per unit comoving volume we find, if $\alpha \neq 1$, $S(t) = S_c + (4/3)\kappa A^3\widehat{\rho}^{3/4}t^{3(\alpha-1)}$, and the corresponding proper entropy density is $s(t) = S_c/(A^3t^{3\alpha}) + 4\kappa\widehat{\rho}^{3/4}/(3t^3)$. For the discussion of the entropy we must distinguish three qualitatively different cases.

(i) The case $\alpha > 1$, i.e., $1/2 < \Omega^*_{\bar{\lambda}} < 1$: Here $\mathscr{P}(t) > 0$ so that the entropy and energy content of the matter system increases with time. By Eq. (8.81), $\mathscr{P} > 0$ implies $\dot{\bar{\lambda}} + 8\pi\rho\dot{G} < 0$. Since $\dot{\bar{\lambda}} < 0$ but $\dot{G} > 0$ in the NGFP regime, the energy exchange is predominantly due to the decrease of $\bar{\lambda}$ while the increase of G is subdominant in this respect. The comoving entropy $S(t)$ has a finite limit for $t \to 0$, $S(t \to 0) = S_c$, and $S(t)$ grows monotonically for $t > 0$. If $S_c = 0$, which would be the most natural value in view of the discussion above, *all* of the entropy carried by the matter fields is due to the energy injection from $\bar{\lambda}$.

(ii) The case $\alpha < 1$, i.e., $0 < \Omega^*_{\bar{\lambda}} < 1/2$: Here $\mathscr{P}(t) < 0$ so that the energy and entropy of matter decreases. Since $\mathscr{P} < 0$ amounts to $\dot{\bar{\lambda}} + 8\pi\rho\dot{G} > 0$, the dominant physical effect is the increase of G with time, the counteracting decrease of $\bar{\lambda}$ is less important. The comoving entropy starts out from an infinitely positive value at the initial singularity, $S(t \to 0) \to +\infty$. This case is unphysical probably.

(iii) The case $\alpha = 1$, $\Omega^*_{\bar{\lambda}} = 1/2$: Here $\mathscr{P}(t) \equiv 0$, $S(t) = \text{const}$. The effect of a decreasing $\bar{\lambda}$ and increasing G cancels exactly.

At lower scales the RG trajectory leaves the NGFP and very rapidly 'crosses over' to the GFP. This is most clearly seen in the behavior of the anomalous dimension $\eta_N(k) \equiv k\partial_k \ln G(k)$ which changes from its NGFP value $\eta_* = -2$ to the classical $\eta_N = 0$. This transition happens near $k \approx m_{Pl}$ or, since $k(t) \approx H(t)$, near a cosmological 'transition' time t_{tr} defined by the condition $k(t_{tr}) = \xi H(t_{tr}) = m_{Pl}$. (Recall that $\xi = O(1)$.) The complete solution to the improved equations can be found with numerical methods only. It proves convenient to use logarithmic variables normalized with respect to their respective values at the turning point. Beside the 'RG time' $\tau \equiv \ln(k/k_T)$, we use $x \equiv \ln(a/a_T)$, $y \equiv \ln(t/t_T)$, and $\mathscr{U} \equiv \ln(H/H_T)$.

Summarizing the numerical results, one can say that for any value of $\Omega^*_{\bar{\lambda}}$ the UV cosmologies consist of two scaling regimes and a relatively sharp crossover region near $k, H \approx m_{Pl}$ corresponding to $x \approx -34.5$ which connects them. At higher k-scales the fixed point approximation is valid, at lower scales one has a classical FRW cosmology in which $\bar{\lambda}$ can be neglected.

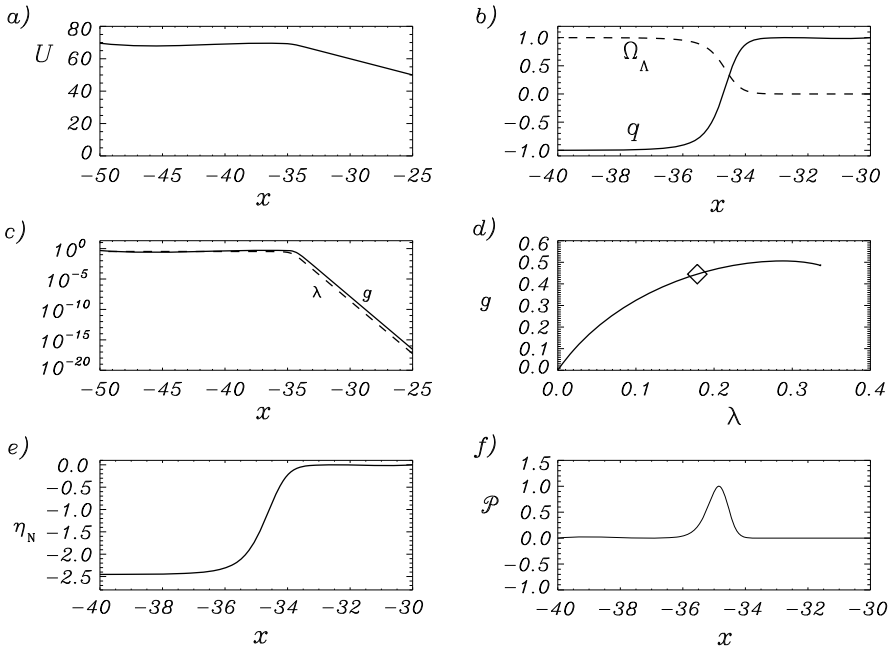

Fig. 8.9 The crossover epoch of the cosmology for $\Omega_{\bar{\lambda}}^* = 0.98$. The plots (**a**), (**b**), (**c**) display the logarithmic Hubble parameter $\mathscr{U}$, as well as q, $\Omega_{\bar{\lambda}}$, g and λ as a function of the logarithmic scale factor x. A crossover is observed near $x \approx -34.5$. The *diamond* in plot (**d**) indicates the point on the RG trajectory corresponding to this x-value. (The lower horizontal part of the trajectory is not visible on this scale.) The plots (**e**) and (**f**) show the x-dependence of the anomalous dimension and entropy production rate, respectively

As an example, Fig. 8.9 shows the crossover cosmology with $\Omega_{\bar{\lambda}}^* = 0.98$ and $w = 1/3$. The entropy production rate $\mathscr{P}$ has a maximum at $t_{\rm tr}$ and quickly goes to zero for $t > t_{\rm tr}$; it is non-zero for all $t < t_{\rm tr}$. By varying the $\Omega_{\bar{\lambda}}^*$-value one can check that the early cosmology is indeed described by the NGFP solution (8.71). For the logarithmic H vs. a plot, for instance, it predicts $\mathscr{U} = -2(1 - \Omega_{\bar{\lambda}}^*)x$ for $x < -34.4$. The left part of the plot in Fig. 8.9a and its counterparts with different values of $\Omega_{\bar{\lambda}}^*$ indeed comply with this relation. If $\Omega_{\bar{\lambda}}^* \in (1/2, 1)$ we have $\alpha = (2 - 2\Omega_{\bar{\lambda}}^*)^{-1} > 1$ and $a(t) \propto t^\alpha$ describes a phase of accelerated power-law inflation.

When $\Omega_{\bar{\lambda}}^* \nearrow 1$ the slope of $\mathscr{U}(x) = -2(1 - \Omega_{\bar{\lambda}}^*)x$ decreases and finally vanishes at $\Omega_{\bar{\lambda}}^* = 1$. This limiting case corresponds to a constant Hubble parameter, i.e., to de Sitter space. For values of $\Omega_{\bar{\lambda}}^*$ smaller than, but close to 1 this de Sitter limit is approximated by an expansion $a \propto t^\alpha$ with a very large exponent α. The phase of power-law inflation automatically comes to a halt once the RG running has reduced $\bar{\lambda}$ to a value where the resulting vacuum energy density no longer can overwhelm the matter energy density.

8.11 Conclusions

In these lectures we reviewed the basic ideas of asymptotic safety and explained why we believe that quantum Einstein gravity is likely to be renormalizable in the modern non-perturbative sense. We argued that the scale-dependence of the gravitational couplings intrinsic to asymptotic safety gives rise to multi-fractal features of the effective space-times and should also have an impact on the cosmological evolution of the Universe we live in. In the latter context, we proposed three possible candidate signatures: a period of automatic, cosmological constant-driven inflation that requires no *ad hoc* inflaton, the entropy carried by the radiation which fills the Universe today, and the primordial density perturbations necessary for structure formation. If these perturbations are an imprint of the metric fluctuations in the NGFP regime, the 'critical phenomenon' properties of the latter might be the origin of the observed scale free spectrum of the former. It is indeed an exciting idea that what we see when we look at the starry sky, during a clear summer night on the Cycladic Islands, for instance, might actually be a snapshot of the geometry fluctuations governed by the short-distance limit of QEG, and tremendously magnified by the cosmic expansion.

Acknowledgements M.R. would like to thank the organizers of the 6th Aegean Summer School for the opportunity to present this material and their cordial hospitality at Naxos. We are also grateful to D. Benedetti and J. Henson for sharing their Monte Carlo data with us, and A. Nink for a careful reading of the manuscript. The research of F.S. is supported by the Deutsche Forschungsgemeinschaft (DFG) within the Emmy-Noether program (Grant SA/1975 1-1).

References

1. G. 't Hooft, M.J.G. Veltman, Ann. Henri Poincaré Phys. Theor. A **20**, 69 (1974)
2. M.H. Goroff, A. Sagnotti, Phys. Lett. B **160**, 81 (1985)
3. A.E.M. van de Ven, Nucl. Phys. B **378**, 309 (1992)
4. M. Niedermaier, M. Reuter, Living Rev. Relativ. **7**, 9 (2006). http://www.livingreviews.org/lrr-2006-5
5. M. Reuter, F. Saueressig, in *Geometric and Topological Methods for Quantum Field Theory*, ed. by H. Ocampo, S. Paycha, A. Vargas (Cambridge University Press, Cambridge, 2010). arXiv:0708.1317
6. R. Percacci, in *Approaches to Quantum Gravity*, ed. by D. Oriti (Cambridge University Press, Cambridge, 2009). arXiv:0709.3851
7. S. Weinberg, in *General Relativity, an Einstein Centenary Survey*, ed. by S.W. Hawking, W. Israel (Cambridge University Press, Cambridge, 1979)
8. S. Weinberg, in *Conceptual Foundations of Quantum Field Theory*, ed. by T.Y. Cao (Cambridge University Press, Cambridge, 1999), pp. 241–251. hep-th/9702027
9. S. Weinberg, arXiv:0903.0568
10. S. Weinberg, PoS CD **09**, 001 (2009). arXiv:0908.1964
11. M. Reuter, Phys. Rev. D **57**, 971 (1998). hep-th/9605030
12. D. Dou, R. Percacci, Class. Quantum Gravity **15**, 3449 (1998). hep-th/9707239
13. O. Lauscher, M. Reuter, Phys. Rev. D **65**, 025013 (2002). hep-th/0108040
14. M. Reuter, F. Saueressig, Phys. Rev. D **65**, 065016 (2002). hep-th/0110054
15. O. Lauscher, M. Reuter, Phys. Rev. D **66**, 025026 (2002). hep-th/0205062

16. O. Lauscher, M. Reuter, Class. Quantum Gravity **19**, 483 (2002). hep-th/0110021
17. O. Lauscher, M. Reuter, Int. J. Mod. Phys. A **17**, 993 (2002). hep-th/0112089
18. W. Souma, Prog. Theor. Phys. **102**, 181 (1999). hep-th/9907027
19. M. Reuter, F. Saueressig, Phys. Rev. D **66**, 125001 (2002). hep-th/0206145
20. M. Reuter, F. Saueressig, Fortschr. Phys. **52**, 650 (2004). hep-th/0311056
21. A. Bonanno, M. Reuter, J. High Energy Phys. **0502**, 035 (2005). hep-th/0410191
22. R. Percacci, D. Perini, Phys. Rev. D **67**, 081503 (2003). hep-th/0207033
23. R. Percacci, D. Perini, Phys. Rev. D **68**, 044018 (2003). hep-th/0304222
24. D. Perini, Nucl. Phys. Proc. Suppl. **127C**, 185 (2004). hep-th/0305053
25. A. Codello, R. Percacci, Phys. Rev. Lett. **97**, 221301 (2006). hep-th/0607128
26. D. Litim, Phys. Rev. Lett. **92**, 201301 (2004). hep-th/0312114
27. P. Fischer, D. Litim, Phys. Lett. B **638**, 497 (2006). hep-th/0602203
28. R. Percacci, D. Perini, Class. Quantum Gravity **21**, 5035 (2004). hep-th/0401071
29. R. Percacci, J. Phys. A **40**, 4895 (2007). hep-th/0409199
30. A. Codello, R. Percacci, C. Rahmede, Int. J. Mod. Phys. A **23**, 143 (2008). arXiv:0705.1769
31. P.F. Machado, F. Saueressig, Phys. Rev. D **77**, 124045 (2008). arXiv:0712.0445
32. A. Codello, R. Percacci, C. Rahmede, Ann. Phys. **324**, 414 (2009). arXiv:0805.2909
33. M. Reuter, H. Weyer, Phys. Rev. D **79**, 105005 (2009). arXiv:0801.3287
34. M. Reuter, H. Weyer, Gen. Relativ. Gravit. **41**, 983 (2009). arXiv:0903.2971
35. M. Reuter, H. Weyer, Phys. Rev. D **80**, 025001 (2009). arXiv:0804.1475
36. P.F. Machado, R. Percacci, Phys. Rev. D **80**, 024020 (2009). arXiv:0904.2510
37. J.E. Daum, M. Reuter, Adv. Sci. Lett. **2**, 255 (2009). arXiv:0806.3907
38. D. Benedetti, P.F. Machado, F. Saueressig, Mod. Phys. Lett. A **24**, 2233 (2009). arXiv:0901.2984
39. D. Benedetti, P.F. Machado, F. Saueressig, Nucl. Phys. B **824**, 168 (2010). arXiv:0902.4630
40. D. Benedetti, P.F. Machado, F. Saueressig, arXiv:0909.3265
41. J.-E. Daum, U. Harst, M. Reuter, J. High Energy Phys. **1001**, 084 (2010). arXiv:0910.4938
42. U. Harst, M. Reuter, J. High Energy Phys. **1105**, 119 (2011). arXiv:1101.6007
43. A. Eichhorn, H. Gies, M.M. Scherer, Phys. Rev. D **80**, 104003 (2009). arXiv:0907.1828
44. K. Groh, F. Saueressig, J. Phys. A **43**, 365403 (2010). arXiv:1001.5032
45. A. Eichhorn, H. Gies, Phys. Rev. D **81**, 104010 (2010). arXiv:1001.5033
46. E. Manrique, M. Reuter, Ann. Phys. **325**, 785 (2010). arXiv:0907.2617
47. E. Manrique, M. Reuter, F. Saueressig, Ann. Phys. **326**, 440 (2011). arXiv:1003.5129
48. E. Manrique, M. Reuter, F. Saueressig, Ann. Phys. **326**, 463 (2011). arXiv:1006.0099
49. E. Manrique, M. Reuter, Phys. Rev. D **79**, 025008 (2009). arXiv:0811.3888
50. E. Manrique, S. Rechenberger, F. Saueressig, Phys. Rev. Lett. **106**, 251302 (2011). arXiv:1102.5012
51. J.-E. Daum, M. Reuter, Phys. Lett. B **710**, 215 (2012). arXiv:1012.4280
52. J.-E. Daum, M. Reuter, PoS **CNCFG 2010**, 003 (2010). arXiv:1111.1000
53. D. Benedetti, K. Groh, P.F. Machado, F. Saueressig, J. High Energy Phys. **1106**, 079 (2011). arXiv:1012.3081
54. M. Niedermaier, Phys. Rev. Lett. **103**, 101303 (2009)
55. K. Groh, S. Rechenberger, F. Saueressig, O. Zanusso, PoS EPS **-HEP2011**, 124 (2011). arXiv:1111.1743
56. D. Benedetti, New J. Phys. **14**, 015005 (2012). arXiv:1107.3110
57. P. Forgács, M. Niedermaier, hep-th/0207028
58. M. Niedermaier, J. High Energy Phys. **0212**, 066 (2002). hep-th/0207143
59. M. Niedermaier, Nucl. Phys. B **673**, 131 (2003). hep-th/0304117
60. M. Niedermaier, Class. Quantum Gravity **24**, R171 (2007). gr-qc/0610018
61. C. Wetterich, Phys. Lett. B **301**, 90 (1993)
62. M. Reuter, C. Wetterich, Nucl. Phys. B **417**, 181 (1994)
63. M. Reuter, C. Wetterich, Nucl. Phys. B **427**, 291 (1994)
64. M. Reuter, C. Wetterich, Nucl. Phys. B **391**, 147 (1993)
65. M. Reuter, C. Wetterich, Nucl. Phys. B **408**, 91 (1993)

66. M. Reuter, Phys. Rev. D **53**, 4430 (1996). hep-th/9511128
67. M. Reuter, Mod. Phys. Lett. A **12**, 2777 (1997). hep-th/9604124
68. J. Berges, N. Tetradis, C. Wetterich, Phys. Rep. **363**, 223 (2002). hep-ph/0005122
69. C. Wetterich, Int. J. Mod. Phys. A **16**, 1951 (2001). hep-ph/0101178
70. M. Reuter, hep-th/9602012
71. J. Pawlowski, Ann. Phys. **322**, 2831 (2007). hep-th/0512261
72. H. Gies, hep-ph/0611146
73. C. Bagnuls, C. Bervillier, Phys. Rep. **348**, 91 (2001). hep-th/0002034
74. T.R. Morris, Prog. Theor. Phys. Suppl. **131**, 395 (1998). hep-th/9802039
75. J. Polonyi, Cent. Eur. J. Phys. **1**, 1 (2004)
76. O.J. Rosten, Phys. Rep. **511**, 177 (2012). arXiv:1003.1366
77. A. Bonanno, M. Reuter, Phys. Rev. D **65**, 043508 (2002). hep-th/0106133
78. M. Reuter, F. Saueressig, J. Cosmol. Astropart. Phys. **0509**, 012 (2005). hep-th/0507167
79. A. Bonanno, M. Reuter, J. Phys. Conf. Ser. **140**, 012008 (2008). arXiv:0803.2546
80. A. Bonanno, M. Reuter, J. Cosmol. Astropart. Phys. **0708**, 024 (2007). arXiv:0706.0174
81. A. Bonanno, M. Reuter, Entropy **13**, 274 (2011). arXiv:1011.2794
82. M. Reuter, J. Schwindt, J. High Energy Phys. **0601**, 070 (2006). hep-th/0511021
83. M. Reuter, J. Schwindt, J. High Energy Phys. **0701**, 049 (2007). hep-th/0611294
84. B. Mandelbrot, *The Fractal Geometry of Nature* (Freeman, New York, 1977)
85. H. Kawai, M. Ninomiya, Nucl. Phys. B **336**, 115 (1990)
86. R. Floreanini, R. Percacci, Nucl. Phys. B **436**, 141 (1995). hep-th/9305172
87. I. Antoniadis, P.O. Mazur, E. Mottola, Phys. Lett. B **444**, 284 (1998). hep-th/9808070
88. J. Ambjørn, J. Jurkiewicz, R. Loll, Phys. Rev. Lett. **93**, 131301 (2004). hep-th/0404156
89. J. Ambjørn, J. Jurkiewicz, R. Loll, Phys. Lett. B **607**, 205 (2005). hep-th/0411152
90. J. Ambjørn, J. Jurkiewicz, R. Loll, Phys. Rev. Lett. **95**, 171301 (2005). hep-th/0505113
91. J. Ambjørn, J. Jurkiewicz, R. Loll, Phys. Rev. D **72**, 064014 (2005). hep-th/0505154
92. J. Ambjørn, J. Jurkiewicz, R. Loll, Contemp. Phys. **47**, 103 (2006). hep-th/0509010
93. J. Ambjørn, S. Jordan, J. Jurkiewicz, R. Loll, Phys. Rev. Lett. **107**, 211303 (2011). arXiv:1108.3932
94. D. Benedetti, J. Henson, Phys. Rev. D **80**, 124036 (2009). arXiv:0911.0401
95. R. Kommu, arXiv:1110.6875
96. J. Ambjørn, J. Jurkiewicz, R. Loll, Lect. Notes Phys. **807**, 59 (2010). arXiv:0906.3947
97. O. Lauscher, M. Reuter, J. High Energy Phys. **0510**, 050 (2005). hep-th/0508202
98. J. Laiho, D. Coumbe, Phys. Rev. Lett. **107**, 161301 (2011). arXiv:1104.5505
99. M. Reuter, F. Saueressig, J. High Energy Phys. **1112**, 012 (2011). arXiv:1110.5224
100. L. Modesto, Class. Quantum Gravity **26**, 242002 (2009). arXiv:0812.2214
101. L. Modesto, arXiv:0905.1665
102. F. Caravelli, L. Modesto, arXiv:0905.2170
103. E. Magliaro, C. Perini, L. Modesto, arXiv:0911.0437
104. S. Carlip, AIP Conf. Proc. **1196**, 72 (2009). arXiv:0909.3329
105. S. Carlip, in *Foundations of Space and Time*, ed. by G. Ellis, J. Murugan, A. Weltman (Cambridge University Press, Cambridge, 2012). arXiv:1009.1136
106. S. Carlip, D. Grumiller, Phys. Rev. D **84**, 084029 (2011). arXiv:1108.4686
107. A. Connes, J. High Energy Phys. **0611**, 081 (2006). hep-th/0608226
108. A.H. Chamseddine, A. Connes, M. Marcolli, Adv. Theor. Math. Phys. **11**, 991 (2007). hep-th/0610241
109. D. Guido, T. Isola, J. Funct. Anal. **203**, 362 (2003). math.OA/0202108
110. D. Guido, T. Isola, in *Advances in Operator Algebras and Mathematical Physics*, ed. by F. Boca, O. Bratteli, R. Longo, H. Siedentop (Theta, Bucharest, 2005). math.OA/0404295
111. C. Antonescu, E. Christensen, math.OA/0309044
112. D. Benedetti, Phys. Rev. Lett. **102**, 111303 (2009). arXiv:0811.1396
113. T.P. Sotiriou, M. Visser, S. Weinfurtner, Phys. Rev. Lett. **107**, 131303 (2011). arXiv:1105.5646
114. G. Calcagni, Phys. Rev. Lett. **104**, 251301 (2010). arXiv:0912.3142

115. G. Calcagni, J. High Energy Phys. **1003**, 120 (2010). arXiv:1001.0571
116. G. Calcagni, Phys. Lett. B **697**, 251 (2011). arXiv:1012.1244
117. M. Arzano, G. Calcagni, D. Oriti, M. Scalisi, Phys. Rev. D **84**, 125002 (2011). arXiv:1107.5308
118. G. Calcagni Adv. Theor. Math. Phys. (to be published). arXiv:1106.5787
119. G. Calcagni, J. High Energy Phys. **1201**, 065 (2012). arXiv:1107.5041
120. E. Akkermans, G.V. Dunne, A. Teplyaev, Phys. Rev. Lett. **105**, 230407 (2010). arXiv:1010.1148
121. E. Akkermans, G.V. Dunne, A. Teplyaev, Europhys. Lett. **88**, 40007 (2009). arXiv:0903.3681
122. C.T. Hill, Phys. Rev. D **67**, 085004 (2003). hep-th/0210076
123. A. Bonanno, M. Reuter, Phys. Rev. D **62**, 043008 (2000). hep-th/0002196
124. A. Bonanno, M. Reuter, Phys. Rev. D **73**, 083005 (2006). hep-th/0602159
125. A. Bonanno, M. Reuter, Phys. Rev. D **60**, 084011 (1999). gr-qc/9811026
126. M. Reuter, E. Tuiran, Phys. Rev. D **83**, 044041 (2011). arXiv:1009.3528
127. A. Bonanno, M. Reuter, Phys. Lett. B **527**, 9 (2002). astro-ph/0106468
128. A. Bonanno, M. Reuter, Int. J. Mod. Phys. D **13**, 107 (2004). astro-ph/0210472
129. E. Bentivegna, A. Bonanno, M. Reuter, J. Cosmol. Astropart. Phys. **0401**, 001 (2004). astro-ph/0303150
130. S. Weinberg, Phys. Rev. D **81**, 083535 (2010). arXiv:0911.3165
131. M. Reuter, H. Weyer, Phys. Rev. D **69**, 104022 (2004). hep-th/0311196
132. M. Reuter, H. Weyer, Phys. Rev. D **70**, 124028 (2004). hep-th/0410117
133. M. Reuter, H. Weyer, J. Cosmol. Astropart. Phys. **0412**, 001 (2004). hep-th/0410119
134. B.F.L. Ward, Mod. Phys. Lett. A **23**, 3299 (2008). arXiv:0808.3124
135. A. Bonanno, A. Contillo, R. Percacci, Class. Quantum Gravity **28**, 145026 (2011). arXiv:1006.0192
136. M. Hindmarsh, D. Litim, C. Rahmede, J. Cosmol. Astropart. Phys. **1107**, 019 (2011). arXiv:1101.5401
137. J. Hewett, T. Rizzo, J. High Energy Phys. **0712**, 009 (2007). arXiv:0707.3182
138. D.F. Litim, T. Plehn, Phys. Rev. Lett. **100**, 131301 (2008). arXiv:0707.3983
139. B. Koch, Phys. Lett. B **663**, 334 (2008). arXiv:0707.4644
140. K. Falls, D.F. Litim, A. Raghuraman, Int. J. Mod. Phys. A **27**, 1250019 (2012). arXiv:1002.0260
141. B.S. DeWitt, *The Global Approach to Quantum Field Theory* (Clarendon Press, Oxford, 2003)
142. D. ben-Avraham, S. Havlin, *Diffusion and Reactions in Fractals and Disordered Systems* (Cambridge University Press, Cambridge, 2004)
143. S. Alexander, R. Orbach, J. Phys. Lett. (Paris) **43**, L625 (1982)
144. J.A.S. Lima, Phys. Rev. D **54**, 2571 (1996). gr-qc/9605055
145. J.A.S. Lima, Gen. Relativ. Gravit. **29**, 805 (1997). gr-qc/9605056